Isospin dependence of nucleon-nucleon cross-section in heavy ion reactions

A thesis submitted in partial fulfillment of the requirement for
the award of the degree of

Masters of Science
In
PHYSICS

Under
the supervsion of

Dr. Suneel Kumar

Submitted by

Supreet
Roll no. - 30704019

School of Physics and Materials Science
Thapar University
Patiala – 147004 (PUNJAB)

INDIA

CERTIFICATE

This is to certify that Ms. Supreet, Roll No. 30704019 has worked on this thesis report as a partial fulfillment for award of the degree of **MASTERS OF SCIENCE** in physics. I certify that the matter embodied in this report is of candidate's own record and not submitted to any other university in any part or full form for the award of such a degree.

(Dr. Suneel Kumar)
Supervisor
SPMS, Thapar University
Patiala.

Countersigned by:

Dr. O.P. Pandey
(Prof. & Head)
School of Physics and Materials Science,
Thapar University,
Patiala.

Dr. R.K. Sharma
Dean of academic Affairs
Thapar University,
Patiala.

Acknowledgement

I owe my deepest gratitude to **Dr. Suneel Kumar**, *my worthy supervisor*, who has been an inspiration during my research work. Without him, this thesis would not have been possible. I thank him for his patience and encouragement that carried me on through difficult times, and for his insights and suggestions that helped to shape my research skills. I express my sincere thanks to him for his valuable guidance in carrying out work under his effective supervision, encouragement and cooperation. His visionary thoughts have influenced me greatly. His dynamical attitude has empowered me with a zeal of energy to conquer the minor details of my research work.

I also thank **Dr. O. P. Pandey**, Professor and Head, School of Physics and Material Science for his support and providing facilities.

A special word of thanks to **Mr. Sanjeev Kumar and Mrs. Varinderjit Kaur**, Research Scholars for the help and valuable suggestions whenever I needed out of their busy schedule.

Special thanks are due to all my friends and the staffs at the School of Physics and Material Sciences for providing me a friendly atmosphere and encouraging me throughout this work.

I am deeply thankful to my Family, their moral support and patience has bared fruit through completion of this Thesis.

Supreet

Roll no. 30704019

Date:

ABSTARCT

The rapid progress in producing energetic radioactive beams has offered an excellent opportunity to investigate various isospin effects in the dynamics of nuclear reaction. This study has made it possible to obtain crucial information about the equation of state of isospin asymmetric nuclear matter and the isospin dependent in-medium nucleon nucleon cross-section. Recently, several interesting isospin effects in heavy ion collisions have been explored both experimentally and theoretically. Based on an isospin dependent quantum molecular dynamics model (IQMD), we studied the underlying influence of the isospin effect of nucleon nucleon cross section on the fragmentation, elliptical flow and stopping at intermediate energy heavy-ion collisions. We found the pronounced isospin effects in the nuclear stopping, the multiplicity of intermediate mass fragments and elliptical flow due to mainly the isospin dependent nucleon-nucleon cross-section.

TABLE OF CONTENTS

List of figures

as a function of energy.

CHAPTER 1
Introduction

Atomic nucleus represents one of the fundamental building blocks of the matter in universe. It is placed between the atom and hadron in a chain of basic constituents that stretches from quarks to galaxies. The nucleus has fascinated the mankind since it's discovery. A nucleus consists of a large, but large number of nucleons, interacting via a strong and short range force. The state of a nucleus depends on the temperature and density of it's constituent nucleons. Different dependencies lead to several wonderful and amazing phenomena occuring in nature [1].

1.1 What is Isospin

In physics, and specifically, isospin (isotopic spin, isobaric spin) is a quantum number related to the strong interaction. This term was derived from isotopic spin, but the term isotopic spin is confusing as two isotopes of a nucleus have different numbers of nucleons. Nuclear physicists prefer isobaric spin, which is more precise in meaning. Isospin symmetry is a subset of the flavour symmetry seen more broadly in the interactions of baryons and mesons. Isospin symmetry remains an important concept in particle physics, and a close examination of this symmetry historically led directly to the discovery and understanding of quarks and of the development of Yang-Mills theory. Isospin was introduced by Werner Heisenberg in 1932 (although it was named by Eugene Wigner in 1937 to explain symmetries of newly discovered neutron:

The mass of neutron and proton are almost identical: they are nearly degenerate, and both are thus often called nucleons. Although the proton has a positive charge, and the neutron is neutral, they are almost identical in all other respects.

The strength of the strong interaction between any pair of nucleons is the same, independent of whether they are interacting as protons or as neutrons. Thus, isospin

was introduced as a concept well before the development in the 1960s of the quark model which provides us modern understanding of nuclear physics.

The nucleons, baryons of spin ½, were grouped together because they both have nearly the same mass and interact in nearly the same way. Thus, it was convenient to treat them as being different states of the same particle. Since a spin ½ particle has two states, the two were said to be of isospin ½. The proton and neutron were then associated with different isospin projections $I_z = +1/2$ and $-1/2$ respectively. When constructing a physical theory of nuclear forces, one could then simply assume that it does not depend on isospin.

1.2 Isospin symmetry

In quantum mechanics, when a Hamiltonian has symmetry, that symmetry manifests itself through a set of states that have the same energy; that is, the states are degenerate. In particle physics, the near mass-degeneracy of the neutron and proton points to an approximate symmetry of the Hamiltonian describing the strong interactions. The neutron does have a slightly higher mass due to isospin breaking; this is due to the difference in the masses of the up and down quarks and the effects of the electromagnetic interaction. However, the appearance of an approximate symmetry is still useful, since the small breakings can be described by a perturbation theory, which gives rise to slight differences between the near-degenerate states [2].

1.3 Nuclear physics at intermediate energy

The nuclear physics (at low/intermediate/high energies) is one the most extensively studied field. After many decades, the nuclear physics has reached a moment or critical differentiation. In last two decades, a lot of efforts have been made experimentally as well as theoretical to understand the nuclear physics at intermediate energies which ranges between 10 AMeV and 2 AGeV [3].

With the passage of time, one was able to accelerate the heavy-ion with bombarding energies comparable to its rest mass. This opened up new dimensions which are termed as intermediate and relativistic energy heavy-ion physics. Due to the formation of compressed and hot piece of nuclear mater at intermediate and relativistic energies, it gives possibilities to study the properties of nuclear matter at extreme conditions.

The isospin dependence of in-medium nuclear effective interactions is important for understanding not only novel properties of exotic nuclei near drip lines but also many interesting questions in astrophysics. Especially, it determines the symmetry energy $E_{sym}(\rho)$ term in the equation of state (EOS) of isospin asymmetric nuclear matter. The density-dependent symmetry energy itself is still poorly known but very important for both nuclear physics and astrophysics. Heavy-ion reactions induced by neutron-rich nuclei provide a unique opportunity to explore the isospin dependence of in-medium nuclear effective interactions, especially the symmetry energy, in a broad range of density. This is because the isospin degree of freedom plays an important role in heavy-ion collisions through both the nuclear EOS and the nucleon-nucleon (*NN*) scatterings. In particular, the transport of isospin asymmetry between two colliding nuclei is expected to depend on both the symmetry potential and the in-medium *NN* cross sections [4, 5, 6, and 7].

The knowledge about the state of matter can be understood and correlated via phase diagram of water. The phase diagram of water basically shows the state of water depending on the pressure and temperature as depicted in Fig. 1.1[2]. As seen in the Figure, water can exist in three forms consisting of ice, liquid, or steam. Interestingly, when water reaches it's boiling point, additional heating does not yield higher temperatures. Even liquid-gas phase coexists together. This type of transition between two phases is also called as a “*first order phase transition"*. The importance of phase diagram lies in the fact that it can be used to predict the state of water at a given temperature and pressure. The mathematical relation inferred by this diagram is termed as “equation of state" for water [1, 2].

In a similar fashion, the prediction of the equation of state for a nucleus is an important question. The phase diagram of nuclear matter (that has been predicted theoretically) is shown in Fig. 1.2[8]. In their normal states of lowest energy, nuclei show liquid-like characteristics and have a density of 0.17 nucleons/fm^3. In this low energy regime (i.e. $E_{incident}$ ≤ 20 MeV/nucleon), basic interest is to look for the structure of nuclei. One can also study the phenomenon of fusion-fission [9], cluster-radioactivity [11] as well as halo nuclei [12].

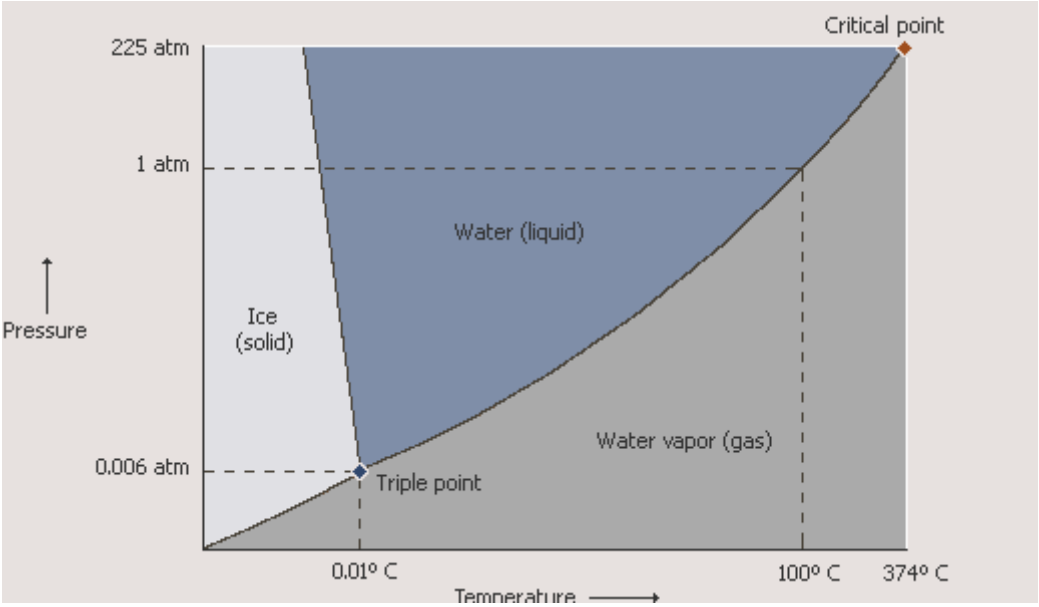

Figure 1.1: Phase diagram of water.

When nucleus is heated to a temperature of a few MeV (1 MeV = 1.2x 10^{10} K), some of the nuclear liquid may also evaporate. Just like water, it also has a latent heat of vaporization leading to a "*first-order phase transition"*. This liquid-gas coexistence is expected to cease at a critical point. The study of nuclear matter under the extreme conditions of temperature and density can be handled by a number of possible candidates listed in Table 1.1[1].

Candidate	Max. Density	Max. Temp.	Comments
Finite nucleus (monopole)	$\rho/\rho_0 \approx 1$	T ≈ 0 MeV	Very small range of density is available
Neutron star	$\rho/\rho_0 \approx 6$	T ≈ 6 MeV	Rare in time and remote in space
Supernova	$\rho/\rho_0 \approx 4$	T ≈ 10 MeV	Rare in time and remote in space
Heavy ion Collisions @ intermediate energies	$\rho/\rho_0 \approx$ 2-3	T ≈ 100 MeV	Give unique possibility to study the matter at high density and temperature.

Table1.1: Different candidates for high densities and temperatures.

One can see from Table 1.1, finite nuclei yield a small range of density only. Other candidates like the neutron stars as well as supernova explosions are far in space and remote in time therefore, are of limited interest only. The best candidate that provides nuclear matter under the extreme conditions in a controlled fashion is the heavy-ion collision at intermediate energies (i.e. 20 MeV/nucleon ≤ *Eincident* ≤ 2 GeV/nucleon). Some of the observed phenomena in this energy domain are transverse flow, multifragmentation and particle production etc.

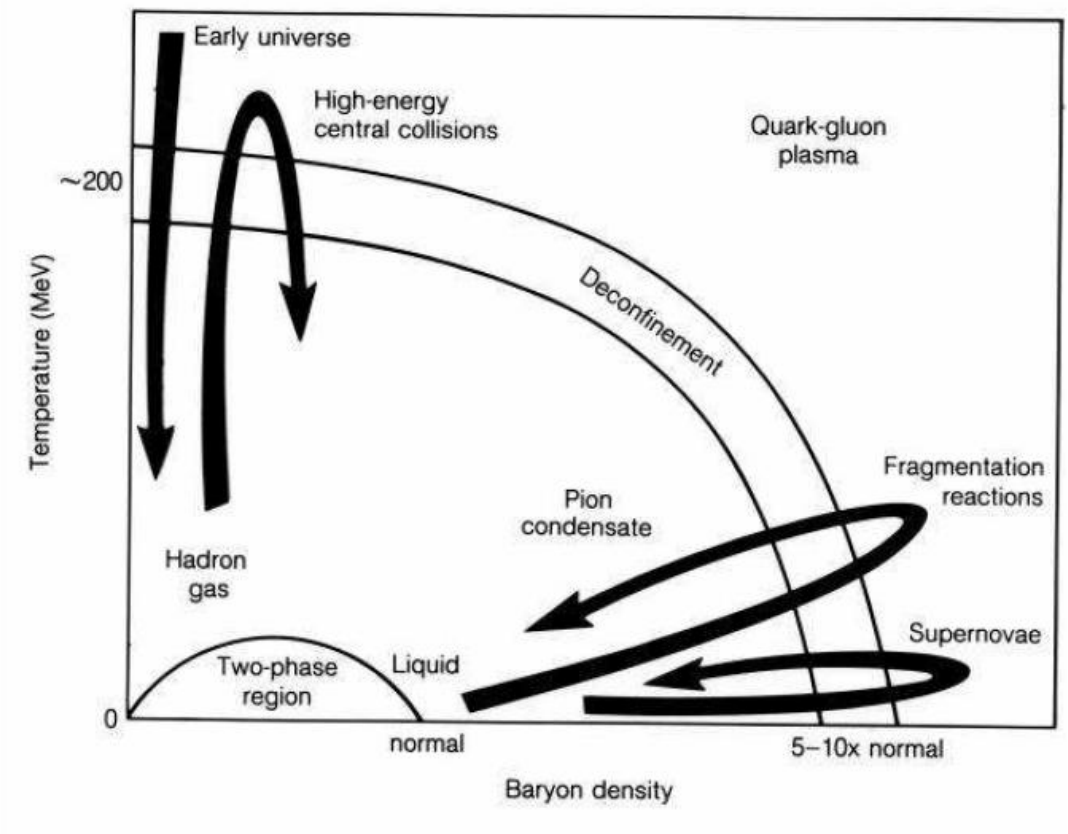

Figure 1.2: Phase diagram of nuclear matter. The theoretical predictions are also displayed at all temperatures. The only experimentally known point is $\rho = \rho_0$ at T = 0. The trajectories of a supernova explosion and of a heavy-ion reaction are also shown.

As indicated in fig 1.2, there are conjunctions about a nuclear liquid-vapour phase transitions at low temperature and sub-nucleonic densities. At very high temperature and densities, one may have the quark gluon plasma, whereas at moderate temperature, the hardon gas occurs.

The rapid progress in producing energetic radioactive beams has offered an excellent opportunity to investigate various isospin effects in the dynamics of nuclear reactions .This study has made it possible to obtain crucial information about the equation of state of isospin asymmetric nuclear matter and about the isospin dependent in-medium nucleon-nucleon cross-section. This information is important for

understanding both novel properties of neutron or proton-rich nuclei as well as explosion mechanisms of supernovae and the cooling rates of proton-neutron stars.

One of the main interests of the study of heavy ion collisions is the investigation of the properties of nuclear matter at extreme densities and excitation energies. These investigations include the production of secondary particles, the properties of particles in a (dense) nuclear medium, the compression and repulsion of dense nuclear matter, its equilibration during the reaction and its decay into fragments and free nucleons. On a macroscopic level the total energy of a dense nuclear system and its decomposition into thermal and compressional parts is related to the concept of the nuclear equation of state. Since a consistent derivation of the nuclear equation of state, e.g. the energy per nucleon as a function of density and temperature is only possible in the low density limit (Bruckner theory) a reliable theoretical description is not at hand. On the other hand this quantity is of interest for many astrophysical questions and therefore its knowledge is highly desirable. Heavy ion reactions in combination with corresponding simulations using a variety of parameterizations of the equation of state are presently the only possible approach to study this quantity.

Heavy ion collisions allow searching for a large number of observables which may be used as indicators of the properties of matter under extreme conditions. Frequently these observables are related to the quantitative description of collective effects like the bounce-off of cold spectator matter in the reaction plane [9] and the squeeze-out of hot and compressed participant matter perpendicular to the reaction plane as well as to the production of secondary particles.

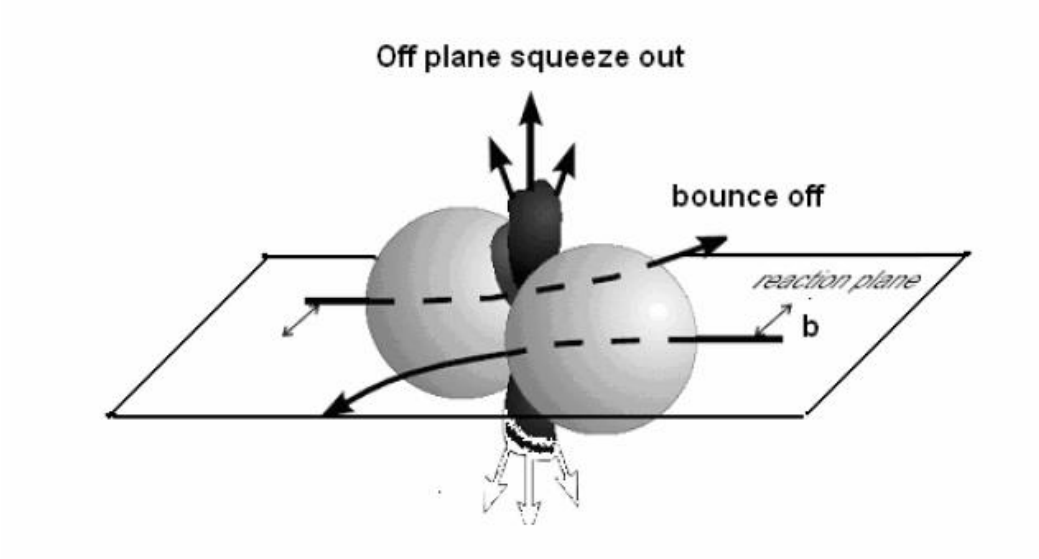

Figure 1.3: Display of the in-plane bounce off caused by compression. and the squeeze out, the enhanced emission of light particles perpendicular to the reaction plane close to midrapidity. Figure is taken from Ref. [12].

1.4 Experimental review

The early natural accelerator available to the mankind was cosmic rays. Cosmic rays consist primarily of protons having share of 85%. In addition, 14% are helium nuclei and remaining 1% is made up of all other heavier elements [13]. The secondary component of cosmic rays is formed when heavier nuclei namely carbon and oxygen collide with interstellar matter. In this process, they break into lighter nuclei like $^{7}Li_{3}$, $^{9}Be_{4}$ and $^{11}B_{5}$. This spallation is also responsible for the abundance of ^{48}Ti, ^{51}V and ^{55}Mn elements in cosmic rays [14]. It was realized later on that the energetic particles obtained in the cosmic rays consist of elements of different masses with different energies leading to inclusive experiments. The exclusive experiments, however, need fixed incident energy as well as mass. This was possible in accelerators only.

Earlier, one could accelerate the light ions only; therefore, the field was dominated by shooting light particles on heavy targets. As the quest grew, new and larger accelerators were built which could accelerate heavy nuclei up to several hundreds of GeV that led to the new unexplored world of nuclear physics. As such, it

represents a rich and challenging world well worthy of intellectual pursuit and its study is important for a deep and a more complete understanding of nature.

One of the earlier accelerators was the *BEVALAC* accelerator at the Lawrance Berkeley Laboratory that led way to high energy accelerators built at the Michigan State University (*MSU*)(*USA*), Grand Accelerateur National D'ions Lourds (*GANIL*) (*France*), Relativistic Heavy-Ion Collider (*RHIC*) and Superconducting Supercollider (*SSC*) at *BNL* (*USA*), *NSF-Arizona* accelerator at the University of Arizona *(USA)*, Vivitron accelerator in Strasbourg *(France)*, Superconducting cyclotron at Texas (*USA*), Superconducting cyclotron at *INFN (Italy)* and the Heavy-ion Synchrotron (*SIS*) accelerator at *GSI (Germany)* etc. These accelerators provide unique possibility to study the heavy-ion collisions in a laboratory under controlled fashion. In actual heavy-ion experiments, the sorting of “well measured" events as a function of the violence of the collision (i.e. impact parameter) is a crucial part of analysis and has to be taken care of before comparing it with the theoretical results. The global variables like Particle Multiplicity (*PM*), ratio of Transversal and Longitudinal Kinetic Energy (*ERAT*), total detected Transverse Energy ($E^{tot}{}_{tr}$), Transverse Energy of light charged particles (E_{trans}12), Total Kinetic Energy Loss (*TKEL*) etc. has been widely used to sort out the events. The multiplicity of charged particles, PM, has often been used by *FOPI* group at *GSI* to characterize events.

The two major groups at *GSI* i.e. *FOPI* and *ALADIN* have provided an important breakthrough on the experimental front to study the phenomena of multifragmentation.
Incidentally, the *ALADIN* group made the first measurements of the nuclear caloric curve [15]. They offered a wide coverage of masses between ^{12}C and ^{208}Pb with incident energy between 100 to 1000 MeV /nucleon [16-18]. The *ALADIN* results are the most complete piece of data available for multifragmentation[16]. In these collisions, energy depositions are reached which cover the range from the particle evaporation to multifragment emission and further to the total disassembly of the nuclear matter. This also led to the so called *“rise and fall"* of multifragmentation . The most striking feature is the *“universality"* that is obeyed by fragment multiplicities and fragment charge

correlations [16]. These observations are invariant with respect to entrance channel and are independent of the beam energy and target if plotted as a function of Z_{bound}; Z_{bound} is the sum of charges of all fragments with Z> 2. The dependence of fragment multiplicity on the projectile mass follows a linear scaling law [16].

The National Superconducting Cyclotron Laboratory of Michigan State University (*MSU*) lay emphasis on the asymmetric reactions like $^{36}Ar+^{197}Au$, $^{129}Xe+^{197}Au$(at 50- 110 MeV/nucleon), $^{129}Xe+^{12}C$, ^{27}Al, ^{51}V , ^{64}Cu, ^{89}Y (at 50 MeV/nucleon), $^{40}Ar+^{197}Au$ (at 35, 50, 80, 110 MeV/nucleon),$^{40}Ar+^{45}Sc$ (at 15-115 MeV/nucleon) [18]. The average multiplicities, spectral slopes, and masses of heaviest fragments are also investigated or central $^{40}Ar+^{64}Cu$, ^{108}Ag, ^{197}Au (at 17-115 MeV/nucleon) collisions [19].

Apart from these observations, the associated property of fragments i.e. transverse flow has also attracted a wide attention. It has been observed that the fragments are found to exhibit larger transverse flow compared to nucleons [20]. The transverse flow depends strongly on the incident energy. At low incident energies, nuclear interactions are dominated by the attractive part of nuclear mean field deflecting the particles to negative angles [21]. In the domain of intermediate energy, the individual nucleon nucleon scattering and the repulsive part of nuclear mean field become prominent and particles are emitted in the positive scattering angles. Therefore, while going from the low incident energy to higher energy, attractive interactions could be balanced by the repulsive Interactions resulting in net zero transverse flow. The energy at which the flow becomes zero is termed in the literature either as the *energy of vanishing flow* (*EVF*) or *balance energy* (E_{bal}) [23]. The first attempt to measure the balance energy was made by the *MSU* group. First systematic study of the mass dependence of the disappearance of flow was done by Westfall *et al.* [50] in which balance energy was measured for $^{12}C+^{12}C$, $^{20}Ne+^{27}Al$, $^{40}Ar+^{45}Sc$, and $^{86}Kr+^{93}Nb$ reactions and was found to scale as A^{τ} ; where A is the mass of the combined system and τ = -1/3 . Magestro *et al. [24]* measured the balance energy for $^{197}Au+^{197}Au$ reaction, thus providing the mass dependence over a wider range. It was found that the

balance energy increases approximately linearly as a function of the impact parameter. The flow of fragment also increases with the size of the fragment at a particular energy or impact parameter [25].

Lots of comparisons have been made between experimental data and microscopic and macroscopic transport theoretical calculations. The theoretical situation is more complicated. There are two different types of models which are widely used and are able to explain one or more features of the experimental results. The first type of model is based on a statistical (and static) approach. These models neglect the dynamics of the collision and hence depend on the excitation energy and density of the composite system only. In this case, the nucleon-nucleon correlations are neglected. The second type of model are dynamical models such as the molecular dynamics models,and one body models such as the Boltzmann-Uhling-Uhlenbeck (BUU).These models simulate the heavy-ion reaction from two well defined initial nuclei to the expansion stage where nuclear matter breaks into several pieces. These models take the complete dynamics of the reaction into account [26].

The dynamics of the reaction is governed by the mean field (or mutual two and three body interactions) and by nucleon nucleon cross-section. Both these ingredient have different domain of dominance. At low energies, the two body collisions are nearly absent and therefore, the mean field (mutual two and three body interaction dominates the reaction where as the nucleon nucleon collisions take over the picture at relativistic energies.

The total reaction cross section σ_R has been extensively studied theoretically and experimentally [27-36]. There are two kinds of theoretical models to calculate σ_R.The first is the low energy theory based on the interaction potential. Such models are not successful for the reaction beyond 10-15 MeV/nucleon above the Coulomb barrier.The second is the high energy microscopic Glauber theory based on the individual nucleon-nucleon collisions in the overlap volume of the projectile and target. However, the roles of mean field and medium effect are difficult to be discussed in the Glauber-type model.

In recent years, Ma et al. developed a new method to study σ_R with helps of transport theory and Glauber model [37]. Originally, the BUU model [38] was taken as a tool to investigate σ_R [37]. Later, the quantum molecular dynamics (QMD) model was applied to study σ_R [39] in the same spirit as Ref [37]. The reaction dynamics in transport theory at intermediate energy is mainly governed by the mean field, two-body collisions, and Pauli blocking. To investigate the isospin effects, the above three dynamical ingredients should include properly isospin degrees of freedom to obtain an isospin quantum molecular dynamics (IQMD). It is also important that the samples of neutrons and protons in the phase space should be treated separately in the initialization of projectile and target nuclei. The IQMD model is introduced to calculate σ_R. This model incorporates the isospin dependence of mean-field, nucleon-nucleon cross section, and Pauli blocking. It has been widely used to study the multi-fragmentation and the collective flow. In the IQMD model, neutrons and protons are distinguishable in the initialization. The density distributions for the initial projectile and target nuclei are determined from the Skyrme-Hartree- Fock (SHF) calculation [40] with parameter set SKM.

1.5 Review of Theoretical models

The key point to remember is that the heavy-ion collisions involve very complicated non-equilibrium physics; therefore, its numerical modeling is not straight for-ward. Due to the lack of free available phase-space at low incident energies, about 98% of the attempted coillisions are blocked. The dynamics at low incident energies, is therefore, governed by the mean field only. On the contrary, the availability of large free phase space at relativistic energies (>2 GeV/nucleon) makes Pauli blocking quite ineffective (roughly 4% collisions are blocked). On the other hand, both the Cascade and mean field pictures emerge at intermediate energies. Here one starts from two (well defined) nuclei and follow the dynamics within dynamical model. These dynamical models, therefore, are capable of studying the detailed reaction phenomena with many-body features. Naturally, the situation at the start of the reaction is non equilibrated and therefore, theoretical models used in these situations should not assume global (or

local) equilibrium. A nucleus- nucleus collision at intermediate energy comprises of three stages [41]:

(i). The first one is the *initial stage* where target and projectile are prepared and boosted towards each other with proper center-of-mass energy.

(ii). In the second stage, reaction happens and matter is compressed. One may also observe a piece of hot and dense nuclear matter. This is called as the *compressional stage*.

(iii). The energy stored during the *compressional stage*, when released, gives rise to transverse in-plane flow and multifragments.

In the next section we will explain some models.

1.6 Objective of present work

In this thesis, we have made an attempt to pin down the role of different isospin dependent nn cross-section on various observables in heavy ion reactions. We stimulated thousands of events for neutron rich systems $^{52}Cr_{24} + {}^{108}Ag_{47}$, $^{45}Sc_{21} + {}^{115}In_{49}$, $^{48}Ti_{22} + {}^{112}Cd_{48}$, $^{59}Co_{27} + {}^{101}Ru_{44}$, $^{72}Ge_{32} + {}^{88}Sr_{38}$, and $^{75}As_{33} + {}^{85}Rb_{37}$.

The total mass of the colliding nuclei is kept fixed i.e. 160, so that there is no mass dependence of the total system. We have increased the size of projectile from lower to higher values to see the effect on multifragmentation and nucleon flow.

Stimulations were carried out for incident energy range between 50 and 300 MeV/ nucleon using soft equation of state. The collision geometry is kept non central

with impact parameter $\hat{b} = 0.3$. We carried out our analysis using isospin quantum molecular (IQMD) model.

We carried out an analysis at three different cross-sections Cugnon, 40 mb, and 55 mb using IQMD model.

1.7 References

[1]. J. K. Dhawan, Ph.D. Thesis, P U Chandigarh (2007).

[2]. Uber den Bau der Atomkerne (Zeitschrift für Physik 77: 1-11) and Physical Review 51: 106-119

[3]. Suneel Kumar, Ph.D. Thesis, P U Chandigarh(1999),

[4]. B. A. Li and L.W. Chen Phys. Rev. C 70, 034610 (2004).

[5]. J. M. Lattimer and M. Prakash, Phys. Rep. 333, 121 (2000) Astro. Phys. J. 550, 426 (2001); Science 304, 536 (2004).

[6]. A. W. Steiner, M. Prakash, J. M. Lattimer, and P. J. Ellis, Phys Rep. 411, 325 (2005).

[7]. RIA Theory Bluebook, RIA theory working group, www.orau. org/ria/RIATG.

[8]. Accelerator and Fusion Research Division, Summary of Activities, LBNL Image Library-Collection, Dec. 1991, p. 7-10.

[9]. J. R. Birkelund, J. R. Huizenga, J. N. De and D. Sperber, Phys. Rev. Lett. 40, 1123 (1978); A. Bonasera, Phys. Rev. C 34, 740 (1986); J. N. De and W. Stocker, Phys. Rev. C 42, R819 (1990); M. M. Majumdar, J. N. De, C. Samanta and S. K. Sammadar, Phys. Rev. C 48, 2093 (1993).

[10]. P. B. Price *et al.*, Phys. Rev. C 46, 1939 (1992); Z. Ren, C. Xu and Z. Wang, Phys. Rev. C 70, 034304 (2004).

[11]. C. Yanhuang, A. Smerzi and M. D. Toro, Phys. Rev. C 50, 2809 (1994); Z. H. Liu, X.Z. Zhang and H. Q. Zhang, Phys. Rev. C 68, 024305 (2003); C. Beck, N. Keeley and A. Diaz-Torres, Phys. Rev. C 75, 054605 (2007).

[12]. N. T. Porlie, Nucl. Phys. A 681, 253 (2001); B. K. Srivastva *et al.*, Phys. Rev. C 65, 054617 (2002); J. B. Elliott *et al.*, Phys. Rev. C 71, 024607 (2005).

[13]. M. B. Gottleib, Phys. Rev. 82, 349 (1951).

[14]. C. Perron, Phys. Rev. C 14, 1108 (1976).

[15].J. Hubele *et al.*, Z. Phys. A 340, 263 (1991).

[16]. C. A. Ogilvie *et al.*, Phys. Rev. Lett. 67, 1214 (1991); J. Hubele *et al.*, Phys. Rev. C 46, R1577 (1992); M. Begemann-Blaich *et al.*, Phys. Rev. C 48, 610 (1993); G. F. Peaslee *et al.*, Phys. Rev. C 49, R2271 (1994); A. S. Botvina *et al.*, Nucl. Phys. A 584, 737 (1995); A. SchÄuttauf *et al.*, Nucl. Phys. A 607, 457 (1996); N. T. B. Stone *et al.*, Phys. Rev. Lett. 78, 2084 (1997); A. S. Botvina *et al.*, Phys. Rev. C 74, 044609 (2006).

[17]. B. de Schauenburg, *et al.*, GSI Rep. 98-1, p. 56 (1997); W. Reisdorf, Nucl. Phys. A 630, 15c (1998); W. Reisdorf, *et al.*, *ibid.* 2000-1, p. 45 (1999); W. Reisdorf, Hirschegg, p. 82 (1999); B. Hong *et al.*, Phys. Rev. C 66, 034901 (2002).

[18]. G. Poggi *et al.*, Nucl. Phys. A 586, 755 (1995); J. Konopka, *et al.*, GSI Rep. 96-1, p. 65 (1995); J. P. Alard, *et al.*, *ibid.* 97-1, p. 54 (1996); N. Bastid, *et al.*, *ibid.* 98-1, p. 54 (1997); A. Andronic, *et al.*, *ibid.* 98-1, p. 55 (1997).

[19]. R. Sun *et al.*, Phys. Rev. C 61, 06160 (2000).

[20]. G. Peilert, H. StÄocker, W. Griener, A. Rosenhauer, A. Bohnet and J. Aichelin, Phys.Rev. C 39, 1402 (1989).

[21]. M. B. Tsang *et al.*, Phys. Rev. Lett. 57, 559 (1986).

[22]. P. Danielewicz and G. Odyniec, Phys. Lett. B 157, 146 (1985); J. W. Harris *et al.* Nucl. Phys. A 471, 241c (1987).

[23]. J. J. Molitoris and H. StÄocker, Phys. Lett. B 162, 47 (1985); G. F. Bertsch, W. G. Lynch and M. B. Tsang, Phys. Lett. B 189, 384 (1987); D. Krofcheck *et al.*, Phys.

[24]. D. J. Magestro *et al.*, Phys. Rev. C 61, 021602(R) (2000).

[25]. R. Pak *et al.*, Phys. Rev. C 54, 2457 (1996); R. Pak *et al.*, Phys. Rev. C 53, R1469 (1996).

[26]. Eur. Phys. J. A 1, 151{169 (1998).

[27]. Shen W Q, Wang B et al 1989 Nucl. Phys A 491130.

[28]. Karol 1975 Phys. Rev. C 11 1203.

[29]. Tanihata I et al 1985 Phys. Lett. B 160 80.

[30]. Kox S et al 1987 Phys. Rev. C 35 1678 and references therein.

[31]. Ma Y G et al 1993 Phys. Lett. B 302 386; Ma Y G et al 1993 Phys. Rev. C 48 850.
[32]. Feng J, Shen W Q, Ma Y G 1993 Phys. Lett. B 305 9 Fang D Q et al 2000 Chin. Phys. Lett. 17 655.
[33]. Perrin C, Kox S et al 1982 Phys. Rev. Lett. 49 1905.
[34]. Brandan M E 1983 J. Phys. G 9 197.
[35]. Buenerd M, Lounis A et al 1984 Nucl. Phys. A 424 313.
[36]. Tanihata I, Hamagaki H et al 1985 Phys. Rev. Lett. 55 2676; Fang D Q, Shen W Q, Feng J, Cai X Z, Ma Y G et al 2001 Chin. Phys. Lett. 18 1033.
[37]. Bertsch G F and Das Gupta S 1998 Phys. Rep. 160 189.
[38]. Zhang X D, Ge L X 1996 High Energ. Nucl. Phys. 20 270 (in Chinese).
[40]. Reinhard P G 1991 Computational Nuclear Physics I ed Langanke K (Berlin: Springer).
[41]. H. StÄocker and W. Greiner, Phys. Rep. 137, 277 (1986); J. Aichelin, Phys. Rep. 202, 233 (1991).

Chapter 2

Methodology

2.1 Introduction

As discussed in Chap. 1, the conventional mean field theories [2] like the Hartree-Fock and Schrödinger equation are suitable for the low energy reactions only. The dynamics at intermediate energy, however, requires the equal weightage to nucleon-nucleon binary collisions and mean field. This demands the correct information about the real and imaginary parts of the potential. In addition, one also has to deal with the initial non-equilibrated situation that changes during the course of the reaction. The dynamical transport models employed at intermediate energies are supposed to include the essential collision physics. The real part influences the trajectory of nucleons whereas the imaginary part deals with the nucleon-nucleon collisions. Presently the microscopic models can be subdivided into two classes: Those which follow the time evolution of the one-body phase space distribution and those which are based on *n*-body molecular dynamics or cascade schemes. We will discuss the Vlasov-Uehling-Uhlenbeck (VUU) model,BUU model, IBUU model, INC model, the Quantum Molecular dynamics (QMD) model and its extension i.e. Isospin Quantum Molecular Dynamic Model (IQMD).

The dynamical models can follow the time evolution of nucleons only. These models are termed as “primary models" which generate the phase-space of nucleons. One needs a procedure to define the clusters. These algorithms are termed as “secondary models". In a very simple picture, nucleons are connected to a cluster using space-correlation method. This method identifies two nucleons in the same fragment if their centroids are less than some distance. This method is also called as *Minimum Spanning Tree (MST)* method. This definition is valid only when the system is dilute and thus, it cannot address the question of mechanism behind the multifragmentation which may happen at high densities. Till today, it is one of the most extensively used methods. Several refinements to this method have been proposed. The failure of *QMD+MST* in

explaining the observed fragment distribution obtained by *ALADIN* group was more pronounced at peripheral collisions. This led to the search of alternative procedures to clusterize the nucleons.

2.2 The Intra Nuclear Cascade (INC) Model

The intra nuclear cascade (INC) theoretical approach was a great success for many years and is still widely used as a rough model of the nuclear collision. The basic INC idea is to view the interaction as a sequence of two-body collisions between the particles involved. However, the INC model does not bind the nucleons in any realistic way and fails to accurately describe the event-by-event data. Furthermore, the INC neglects quantum interference effects and the exact equation solved by the simulation is not known. The intra nuclear cascade (INC) model has been proven to be very successful in the description of the main features of nucleus-nucleus, proton-nucleus and antiproton-nucleus reactions in the GeV range [1-3]. In fact this model provides a good description of the first stage of the reaction process, characterized by hard nucleon-nucleon (or, more generally, baryon-baryon) scatterings, and predicts satisfactorily the high-energy part of particle spectra.

At intermediate energies, the mean field and the two-body nucleon nucleon collisions play an equally important role in evolution of the system. In contrast to TDHF model, the Intra Nuclear Cascade Model is capable of describing the high energy heavy-ion collisions [4]. In this model, the mean field is completely neglected and the nucleon-nucleon (NN) collisions are taken into account without Pauli-Blocking [5-12]. Note that this was the first microscopic dynamical model used to understand the experimental data of heavy-ion collisions [4]. The Cascade model simulates the heavy-ion collisions as a superposition of independent two body NN collisions. Naturally, in the absence of mean field, the nucleons move on straight line trajectories until they collide.

In INC model, each nucleus is considered as a collection of point particle distribution within a sphere without any Fermi momentum. When two nuclei approach each other the position of each nucleon (within a sphere) is assigned by Monte-Carlo sampling. The time evolution is followed by dividing the whole reaction time into the small intervals Δt. Two nucleons are supposed to collide if they pass the point of closest approach within a given time interval. The distance of closest approach d_{max} is $\sqrt{\sigma_{nn}^{t}(\sqrt{s})/\pi}$ with $\sigma_{nn}^{t}(\sqrt{s})$ as the total nucleon-nucleon cross section in their center-of-mass system and $\sqrt{s}$ is the centre-of-mass energy. The colliding particles can also scatter elastically or inelastically. The main processes include:

$$\text{elastic:} \begin{cases} N + N \rightarrow N + N\ (a) \\ N + \Delta \rightarrow N + \Delta\ (b) \\ \Delta + \Delta \rightarrow \Delta + \Delta\ (c) \end{cases} \tag{2.1}$$

$$\text{inelastic:} \begin{cases} N + N \rightarrow N + \Delta\ (d) \\ N + \Delta \rightarrow N + N\ (e) \end{cases} \tag{2.2}$$

The cross-sections for channels (a) and (b) are taken from experiments. The cross section for channel (e) is obtained by detailed balance method. The cross sections for channels (b) and (c) are taken to be same as (a).

At the end of the simulations, all Δ's decay isotropically into nucleons and pions by conserving the charge and Isospin quantum number. In other words, the number of $\Delta's$ at the end or reaction gives the number of pions.

One can also calculate the entropy generated in a nuclear system after the collision. The entropy for non interacting Fermionic system is given by

$$S = -\int d\gamma\ [f \ln f + (1-f)\ln(1-f)] \tag{2.3}$$

Here f is the occupation probability in the phase –space which is given by $= \frac{\dot{N}}{R}$, with R being the total number of events and $\dot{N}$ are the number of the particles in a given cell. The $d\gamma$ is the phase space volume element given by $\int d\gamma = 4\int \frac{d^3 r\ d^3 p}{(2\pi\hbar)^3}$. To calculate the

f, the whole phase space is divided into cells i. the distribution function f is then estimated by relation

$$\acute{f} = \frac{n_i}{R \int_i d\gamma} \tag{2.4}$$

The INC gave excellent opportunity to extract the information about several experimental observables [4]. As the INC does not contain the mean field of nucleons, it is more suitable for high energy experiments. The other models which include the mean field as well as the nucleon-nucleon collisions are based on Boltzmann- Uehling – Uhlenbuck (BUU) equation.

2.3 VUU-type models

The microscopic transport models for the one-body Wigner phase space density distribution obtained different names although they solve the same equation. They differ in the technical realization, i.e. the computer program, and are known as Vlasov Uehling–Uhlenbeck (VUU) model [8, 18] (or BUU [10, 11], LV [11]). They solve the following transport equation for the one-body Wigner density *f*(***r***; ***p***; *t*) in the limit $\hbar \longrightarrow 0$:

$$\frac{\partial f}{\partial t} + v.\nabla_r f - \nabla_r U.\nabla_p f = -\frac{1}{(2\pi)^6}\int d^3\mathrm{p}_2\, d^3\dot{p}_2 d\Omega\, \frac{d\sigma}{d\Omega}\, v_{12} \times \{\left[f\, f_2\, (1-\acute{f}_1)(1-\acute{f}_2) - \acute{f}_1\acute{f}_2\, (1-f)(1-f_2)\right] \times (2\pi)^3\, \delta^3\,(p + p_2 - p_1{}' - p_2{}')\} \tag{2.5}$$

The l.h.s. of this equation is the total differential of f with respect to the time assuming a momentum independent potential U. This potential is calculated self consistently and corresponds to the real part of the Bruckner G-matrix. Usually a Skyrme-parametrization :

$$\mathrm{U} = \alpha\left(\frac{\rho}{\rho_0}\right) + \beta\left(\frac{\rho}{\rho_0}\right)^{\gamma} \tag{2.6}$$

of the real part of the G-matrix is employed, where ρ is the nuclear density which is frequently measured in units of the saturation density ρ_0 of cold nuclear matter. The r.h.s. of Eq. (2.4) contains a Boltzmann collision integral, which is identified with the imaginary part of the G-matrix. This part describes the influence of binary hard-core collisions, where the term with ff_2 describes the loss of particles (in a phase space region) and the term with $f'_1 f'_2$ the gain term due to collisions feeding the considered phase space region. It is supplemented with the Nordheim–Uehling–Uhlenbeck modifications in order to obey the Pauli-principle in the final state of the collisions [18]. The δ-functions assure the conservation of the four-momentum. The cross section σ is normally adjusted to the free nucleon-nucleon scattering. The differences from cross sections calculated from the imaginary part of the Br$\ddot{u}$ckner G-matrix are minor [19] and influence little the observables of a heavy ion collision.

The equation is solved by use of the testparticle method. Here the continuous one-body distribution function f at t = 0 is represented by an ensemble of $n(A_p+A_t)$ pointlike particles. This is often viewed as an ensemble of n parallel events with $A_p + A_t$ physical particles each, where Ap and At denote the number of nucleons in projectile and target, respectively. The l.h.s. of Eq. (2.6) can be regarded as the transport equation (Vlasov-equation) for a distribution of classical particles whose time evolution is governed by Hamilton's equations of motion

$$\dot{p}_\iota = -\frac{\delta\langle H\rangle}{\delta r_i}, \qquad \dot{r}_\iota = \frac{\delta\langle H\rangle}{\delta p_i} \tag{2.7}$$

The testparticles move due to their own, selfconsistently generated mean-field. The r.h.s. is taken into account by additional stochastic scattering similar to the collisions in cascade models [20, 21]. More explicitly the test particle method corresponds to the replacement of the expectation value of a single particle observable

$$\langle O\,(t)\rangle = \int f(r,p,t)\; O(r,p)\; d^3\mathrm{r}d^3p \tag{2.8}$$

by a Monte Carlo integration

$$\langle O\,(t)\rangle \;=\; \frac{1}{n(\,\mathrm{A_T}+\,\mathrm{A_P}\,)}\sum_{i=1}^{n(\,\mathrm{A_T}+\,\mathrm{A_P}\,)} O(r_i\,(t), p_i(t)) \tag{2.9}$$

With $r_i(t)$ and $p_i(t)$ denote the points in phase space which are distributed according to f(r, p, t)

$$f(r,p,t) = \lim_{n\to\infty}\frac{1}{n(\,\mathrm{A_T}+\,\mathrm{A_P}\,)}\sum_{i=1}^{n(\,\mathrm{A_T}+\,\mathrm{A_P}\,)}\delta\big(r-r_i\,(t)\big)\,\delta(p-p_i(t)) \tag{2.10}$$

It is evident that a large number n is necessary to avoid numerical noise. Predictions beyond the one-body level are not feasible although several attempts have been made to relate the (unphysical) numerical noise to physical fluctuations. In practice the number n lies in the range between 15 and 500 and one employs a grid to obtain a smooth phase space density distribution.

The numerical realization can be achieved in various ways. VUU uses a phase space sphere around each particle in order to determine f and a coordinate space sphere to determine ρ and thus U(ρ). This corresponds to a Lagrangian method. On the contrary, BUU uses a fixed grid corresponding to an Eulerian method in hydrodynamics. In both models collisions are treated in a parallel event method, only testparticles of the same events, i.e. the Ap + At test particles with the same index n, can collide. The Landau-Vlasov model determines f by the overlap of several Gaussians. The collisions are performed in a crossedevent (or full ensemble) method where all n(Ap + At) may collide with each other particle with a scaled cross section. For the solution of eq. (2.4), proper boundary conditions have to be specified. In the case of heavy ion reactions, the test particles are distributed according to the density- and (Fermi-) momentum distribution of ground state nuclei. The later are then boosted onto every other with the proper relative momentum. Initially the test particles are randomly distributed in a coordinate space sphere of the radius R = $1.48A^{1/3}$ fm (where A is the atomic number of the nucleus) and in a momentum space sphere of the radius of the corresponding Fermi momentum.

One should keep in mind that the forces acting on the test particles are calculated from the entire distribution including test particles from all events, hence the n parallel events are not independent and event-by-event correlations cannot be analyzed within this one body transport models. In the limit $n \rightarrow \infty$ the distribution of these propagated test particles at the time t represents the one-body distribution function at this time. Any one body observable can be calculated by averaging the values weighted with the distribution function. Hence, VUU type models succeeded in the description of one body observables like collective flow, stopping and particle spectra, but, fluctuations and correlations, such as the formation of fragments or the description of two-particle correlations in relativistic heavy ion collisions, are beyond the scope of a transport model based on a one–body distribution function [16, 17]. Any fluctuation of the observables seen in the Monte Carlo simulation of the one–body distribution function is due to numerical noise and disappears in the limit of a infinite number of test particles.

2.4 IBUU model

The IBUU transport used in the present study treats explicitly protons and neutrons. It also includes an asymmetry term in the nuclear mean-field potential and different scattering cross sections for protons and neutrons. The nuclear mean-field potential is parameterized as: [13]

$$U(\rho, t_z) = U_0(\rho,) + U_{asy}(\rho,, t_z), \qquad (2.11)$$

$$U_0(\rho) = a(\rho/\rho_0) + b(\rho/\rho_0)^{\sigma} \qquad (2.12)$$

$$U_{asy}(\rho,, t_z) = C(\rho_p - \rho_n / \rho_0)t_z \qquad (2.13)$$

In the above, ρ_0 is the normal nuclear matter density; ρ, ρ_n and ρ_p the nucleon, neutron and proton densities, respectively; and t_z equals 1 for proton and -1 for neutron. For the

strength of the asymmetry potential, we take C = 32 MeV.

2.5 Quantum Molecular Dynamics (QMD) Model

The QMD model is a *n*-body theory which simulates heavy ion reactions at intermediate energies on an event by event basis. Taking into account all fluctuations and correlations has basically two advantages: i) many-body processes, in particular the formation of complex fragments are explicitly treated and ii) the model allows for an event-by-event analysis of heavy ion reactions similar to the methods which are used for the analysis of exclusive high acceptance data.

The QMD model[26-30] contains the following ingredients: short-range interaction (hard-core repulsion), stochastic scattering with energy- and angle-dependent cross sections, inelastic collisions, particle production, and Fermi motion of the nucleons in the ground state as well as the consideration of the quantum effect of the Pauli principle.

QMD is a microscopic description of heavy-ion collisions, similar to the Vlasov- like models of the preceding section. In QMD each particle *i* is propagated in phase space by means of a Gaussian wave packet. From these packets the total n-particle distribution function results by superposition

$$f(\vec{r},\vec{p},\mathrm{t}) = \sum_{i=0}^{n} f_i\ (\vec{r_i},\vec{p_i},\mathrm{t}) \tag{2.14}$$

With

$$f_i(\vec{r},\ \vec{p}\ ,\mathrm{t}) = \frac{1}{(\pi\hbar)^2}\ e^{-(\vec{r}-\overrightarrow{r_{i0}}(t))^2\frac{1}{2L}} e^{-(\vec{p}-\vec{p}(t))^2\frac{2L}{\hbar^2}} \tag{2.15}$$

In first instance the fixed width of the Gaussian wave packets $\sqrt{2L}$ in equation (2.14) seems to be problematic. However, it was showed by introducing a time-

dependent complex Gaussian width to a QMD version that the Gaussian packets quickly achieve a width which is constant in time. This happens fast compared to the reaction times of about one hundred fm/c, which are relevant here.

A total Hamiltonian function with a kinetic energy T and a potential energy V results:

$$H = T + V = \sum_i \frac{p_i^2}{2m_i} + \sum_i \sum_{j>i} \int f_i(\vec{r}, \vec{p}, t) V^{ij} f_j(\vec{r'}, \vec{p'}, t)\, d\vec{r}\, d\vec{r'}\, d\vec{p}\, d\vec{p'} \qquad (2.16)$$

The potential in equation (2.15) is the sum of the following specific elementary potentials,

$$V = V_{loc} + V_{Yuk} + V_{Coul} + V_{mdi} \qquad (2.17)$$

with the local hard-core repulsion,

$$V_{loc} = \sum_i \sum_{j>i} t_1\, \delta(\vec{r_i} - \vec{r_j}) + \sum_i \sum_{j>i} \sum_{k>j} t_2\, \delta(\vec{r_i} - \vec{r_j})\, \delta(\vec{r_i} - \vec{r_k}), \qquad (2.18)$$

The Yukawa long-range term,

$$V_{Yuk} = \sum_i \sum_{j>i} t_3 \frac{e^{\frac{|\vec{r_i} - \vec{r_j}|}{a}}}{\frac{|\vec{r_i} - \vec{r_j}|}{a}}, \qquad (2.19)$$

the Coulomb term with only a mean value for the nucleon charge because QMD does not know the isospin of the particles,

$$V_{Coul} = \frac{Z}{A} \sum_i \sum_{j>i} \frac{e^2}{|\vec{r_i} - \vec{r_j}|} \qquad (2.20)$$

and the momentum dependent interacion

$$V_{mdi} = \sum_i \sum_{j>i} t_4 \ln(1 + t_5 (\vec{p_i} - \vec{p_j})^2)\, \delta(\vec{r_i} - \vec{r_j}) \qquad (2.21)$$

Parameters used in equations (2.21) to (2.25) can be found in table 2.1. The parameters are propagated under the total interaction calculated by the Hamiltonian equations of motion:

$$\dot{p}_i = -\frac{\delta\langle H\rangle}{\delta r_i}, \qquad \dot{r}_i = \frac{\delta\langle H\rangle}{\delta p_i} \tag{2.22}$$

(I)QMD parameters	
t_3	15 MeV
t_4	1.57 MeV
t_5	$5x10^{-4}$ MeV^{-2}
t_6	25 MeV
a	1.5 fm

Table 2.1: QMD parameters used in equations (2.16) to (2.21).

2.6 Isospin Quantum Molecular Dynamics Model (IQMD)

Quantum molecular dynamics (QMD) model contains two dynamical ingredients, the density dependent mean field and the in-medium nucleon nucleon cross-section. In order to describe the isospin dependence appropriately, the QMD model should be modified properly. Considering the isospin effects in mean field, two-body collision and Pauli blocking, important modifications in QMD have been made to obtain an isospin dependent quantum molecular dynamics (IQMD). The Isospin-QMD (IQMD) treats the different charge states of nucleons, deltas and pions explicitly, as inherited from the VUU model. IQMD has been used for the analysis of collective flow effects of nucleons and pions. As it has been developed from the VUU-model, its coding is therefore

independent of the original QMD. The isospin degrees of freedom enter into the cross sections (here cross sections of VUU similar to the parametrizations of VerWest and Arndt have been taken, see also) as well as in the Coulomb interactions. The elastic and inelastic cross sections for proton-proton and proton-neutron collisions used in IQMD are shown in Fig. 2.1. The cross section for neutron-neutron collisions is assumed to be equal to the proton-proton cross sections [14].

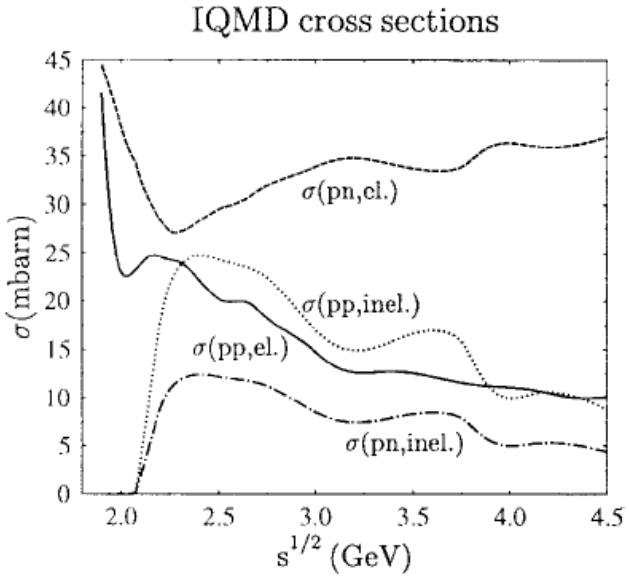

FIG. 2.1. The elastic and inelastic cross sections for proton-proton (pp) and proton neutron (pn) used in IQMD.

A. Potentials used in IQMD

In IQMD particles are represented by the one particle Wigner density [15].

$$f_i(\vec{r},\vec{p},t) = \frac{1}{\pi^3\hbar^3}\; e^{-\left(\vec{r}-\vec{r}_i(t)\right)^2\frac{2}{L}} e^{-\left(\vec{p}-\vec{p}_i(t)\right)^2\frac{L}{2\hbar^2}} \qquad (2.23)$$

The total one particle Wigner density is the sum of all nucleons. The expectation value of the total Hamiltonian is

$$\langle H\rangle = \langle T\rangle + \langle V\rangle$$

$$= \sum_i \frac{p_i^2}{2m_i} + \sum_i \sum_{j>i} \int f_i(\vec{r},\vec{p},t) V^{ij} f_j(\vec{r}',\vec{p}',t)\, d\vec{r}\, d\vec{r}'\, d\vec{p}\, d\vec{p}' \qquad (2.24)$$

The baryon-potential consists of the real part of the G-Matrix which is supplemented by the Coulomb interaction between the charged particles. The former can be further subdivided in a part containing the contact Skyrme-type interaction only, a contribution due to a finite range Yukawa-potential, and a momentum dependent part.

$$V^{ij} = G^{ij} + V_{Coul}^{ij} = V_{Skyrme}^{ij} + V_{Yuk}^{ij} + V_{mdi}^{ij} + V_{Coul}^{ij} + V_{sym}^{ij}$$
$$= t_1\delta(\vec{x}_i - \vec{x}_j) + t_2\delta(\vec{x}_i - \vec{x}_j)\rho^{\gamma-1}(\vec{x}_i) + t_3\frac{exp\{-|\vec{x}_i - \vec{x}_j|/\mu\}}{|\vec{x}_i - \vec{x}_j|/\mu}$$
$$+ t_4 ln^2\left(1 + t_5(\vec{p}_i - \vec{p}_j)^2\right)\delta(\vec{x}_i - \vec{x}_j) + \frac{Z_i Z_j e^2}{|\vec{x}_i - \vec{x}_j|} + t_6\frac{1}{\varrho_0}T_3^i T_3^j\delta(\vec{r}_i$$
$$- \vec{r}_j) \qquad (2.25)$$

The parameters t_1...t_5 are uniquely related to the corresponding values of α, β, γ, δ and ϱ which serve as input. In the calculations presented in this article the parametrization SM is used as standard. It is a combination of Skyrme type and momentum dependent potential with a low compressibility.

In the description of the Coulomb interaction V_{ij}^{coul}, Z_i, Z_j are the charges of the baryons iand j. The momentum dependence of V_{ij}^{mdi} the N–N interaction, which may optionally be used in QMD, is fitted to experimental data [17, 18] on the real part of the nucleon optical potential [19, 20], which yields

$$U_{mdi} = \delta . ln^2(\varepsilon.(\Delta\vec{p})^2 + 1).\left(\frac{\rho_{int}}{\rho_0}\right) \qquad (2.26)$$

The IQMD-model offers rather stable density distributions and good energy conservation, however for the price of nucleon evaporation and and improper binding energies (E_{bind} ≈ 4−5 MeV/nucleon for heavy nuclei instead of 8 MeV/nucleon). In addition to the use of the explicit charge states of all baryons and mesons a symmetry potential between protons and neutrons corresponding to the Bethe-Weizsacker mass formula has been included

$$V_{sym}^{ij} = t_6 \frac{1}{\varrho_0} T_3^i T_3^j \delta(\vec{r}_i - \vec{r}_j) \qquad t_6 = 100MeV \tag{2.27}$$

where T_3^i and T_3^j denote the isospin T_3 of the particles i and j, i.e. 1/2 for protons and -1/2 for neutrons. The potential part of the equation of state resulting from the convolution of the distribution functions f_i and f_j with the interactions V_{ij}^{skyrme}+ V_{ij}^{mdi}(local interactions including momentum dependence) reads:

$$U = \alpha.\left(\frac{\rho_{int}}{\rho_0}\right) + \beta.\left(\frac{\rho_{int}}{\rho_0}\right)^{\gamma} + \delta.ln^2(\varepsilon.(\Delta\vec{p})^2 + 1).\left(\frac{\rho_{int}}{\rho_0}\right) \tag{2.28}$$

B. Collisions

Two particles collide if their minimum distance d, i.e. the minimum relative distance of the centroids of the Gaussians during their motion, in their CM frame fulfills the requirement:

$$d \leq d_0 = \sqrt{\frac{\sigma_{tot}}{\pi}}, \quad \sigma_{tot} = \sigma(\sqrt{s}, type) \tag{2.29}$$

where the cross-section is assumed to be the free cross section of the regarded collision type (N − N, N − Δ, . . .). The total cross-section is the sum of the elastic cross -section and all inelastic cross-sections.

The total cross-section is the sum of the elastic cross-section and all inelastic cross-sections.

$$\sigma_{tot} = \sigma_{el} + \sigma_{inel} = \sigma_{el} + \sum_{channels} \sigma_i \tag{2.28}$$

For instance for a pp collision we may have

$$\sigma_{\mathrm{tot}} = \sigma_{\mathrm{el}} + \sigma(\mathrm{pp} \rightarrow \mathrm{p}\Delta^{+}) + \sigma(\mathrm{pp} \rightarrow \mathrm{n}\Delta^{++}) \tag{2.30}$$

The cross-sections for the different channels are given by experiment or by spin/isospin coefficients. For the pp case for example we have

$$\sigma(pp \to n\Delta^{++}) = 3\sigma(pp \to p\Delta^{+}) = \frac{3}{4}\sigma_{inelastic} \tag{2.31}$$

Inaccessible reactions like $\Delta N \to NN$ are calculated from their reverse reactions (here $NN \to \Delta N$) using detailed balance method. The possibility of reaching a channel in a collision is given by its contribution to the total cross-section

$$P_{channel} = \frac{\sigma_{channel}}{\sigma_{tot}} \qquad e.g. \quad P_{pp\to p\Delta^{+}} = \frac{1}{4}\,\frac{\sigma_{tot} - \sigma_{el}}{\sigma_{tot}} \tag{2.32}$$

C. Initialization in IQMD

In IQMD, the centroids of the Gaussians in a nucleus are randomly distributed in a phase space sphere ($r \le R$ and $p \le p_F$) with $R = 1.48\ A^{1/3}$ fm corresponding to a ground state density of $\rho_0 = 0.17\text{fm}^{-3}$. The Fermi momentum p_F depends on the ground state density. For $\rho_0 = 0.17\text{fm}^{-3}$ it has a value of about $p_F \approx 268$ MeV/c. In IQMD the momenta are uniformly distributed within a momentum sphere $p \le p_{Fermi} \approx 268$ MeV/c without further local constraints. Therefore it may happen that nucleons close to the surface, where the local potential energy is low, are unbound initially. This possibility is not given in BQMD or HQMD. It gives, however, a reduced binding energy per nucleon as compared to the Weizsacker mass formula. Hence the initialized nuclei are less stable against spurious particle evaporation. Finally it should be noted that IQMD performs a Lorentz contraction of the nucleus coordinate distribution which is not present in QMD and which becomes important for higher energies E/nucleon > 1 GeV.

D. Interaction range

As it has already been stated, the Gaussian width can be regarded as a description of the interaction range of a particle. Its influence disappears for infinite nuclear matter whereas for finite systems it may play a non negligible role. In IQMD the Gaussian width can be used as an optional input parameter. The default version uses a system dependent Gaussian width while QMD uses L = 4.33 fm^2 independent of the system size. The system dependence of L in IQMD has been introduced in order to obtain maximum stability of the nucleonic density profiles. As an example for Au+Au a value of L = 8.66 fm^2 is choosen, for Ca+Ca and lighter nuclei L = 4.33 fm^2.

2.7 References

[1] J. Cugnon, Nucl. Phys. A 389, 191c (1982).

[2] J. Cugnon, C. Volant, S. Vuillier, Nucl. Phys. A 625, 729 (1997).

[3] J. Cugnon, J. Vandermeulen, Ann. Phys. (Paris) 14, 49 (1989).

[4] J. Cugnon, T. Mizutani and J. Vandermeulen, Nucl. Phys. A 352, 505 (1981)

[5] S.D. Gupta, C. Gale and J. Gallego, Phys. Rev. C 33, 1634 (1986)

[6] G. Bertsch and J. Cugnon, Phys. Rev. C 24, 2514 (1981)

[7] J. Cugnon and C. Volant, Z. Phys. A 334, 435 (1989)

[8] Y. Yariv and Z. Frankel, Phys. Rev. C 20, 2227 (1979)

[9] Y. Yariv and Z. Frankel, Phys. Rev. C 24, 488 (1981)

[10] J. Cugnon, D. Kinet and J. Vandermeulen, Nucl. Phys. A 379, 553 (1982)

[11] J. Cugnon, Phys. Rev. C 22, 1885 (1980).

[12] J. Cugnon and D. L'Hote, Phys. Lett. B 149, 35 (1984).

[13]. Y. M. Zhenga, C. M. Koa, B. A. Lic, and B. Zhang

[14] Ch. Hatrtnack, Rajeev K. Puri, J. Alchelin..Eur Phys. J. A 1 151-

169(1998).

[15]. C. Hartnack, arXiv:nucl-th/0507002v1 1 Jul 2005

[16] C. Gregoire, B. Remaud, F. Sebille, L. Vinet, and Y. Raffray, Nucl. Phys. A465, 317 (1987).

[17] J. J Molitoris and H. St¨ocker, Phys. Rev C32, R346 (1985).

[18] E. A. Uehling and G. E. Uhlenbeck. Phys. Rev. 43, 552 (1933) and Phys. Rev. 44, 917 (1934).

[19] A. Bohnet et al. Phys. Rev. C44, 2111 (1991).

[20] Y. Yariv and Z. Frankel. Phys. Rev. C20, 2227 (1979).

[21] J. Cugnon. Phys. Rev. C22, 1885 (1980).

Chapter 3

Effect of Isospin on "Collective Flow" in Heavy-Ion Collisions

3.1 Introduction

One of the most sensitive and sought after phenomena at intermediate energy is collective transverse flow. This is also known as in-plane flow. This is also very sensitive to the reaction ingredients and has been investigated extensively over the last two decades. The study of collective flow also gives insight into the reaction dynamics as well as into the hot and dense nuclear matter formed in a reaction. The collective flow was found to be sensitive towards (nuclear matter) equation of state and/or nucleon-nucleon cross-section which is the *the ultimate goal of the intermediate energy heavy-ion collisions*. It depends crucially on several factors such as the size of the system, colliding geometry (i.e impact parameter) and incident energy of the projectile. Collectivity in this context means that a number of ejectiles exhibit a common property (e.g. the emission of many particles of the same kind or the emission of many ejectiles with a common velocity field or into a common direction). Restricting this very general definition of collective behavior to kinematic observables leads to the definition of collective flow: Any common feature of all the ejectiles emitted in a heavy-ion collision can be taken as an indicator for the underlying nuclear-matter phase space distribution. This chapter discusses several collective phenomena, defined as follows:

1. "Longitudinal flow" describes the collective motion of the particles in their original direction defined by the beam.
2. "Radial flow" characterizes particles that are emitted from a source with a common velocity field independent of the direction, i.e. for a velocity field with spherical symmetry.
3. "Transverse flow" is the term used whenever the velocity field is found to be independent of the azimuthal angle.

4. The orientation of the impact parameter vector in nucleus-nucleus collisions defines one specific azimuthal direction. An enhanced emission into this direction is experimentally observed. This most prominent directed flow phenomenon is called “sideflow”.
5. “Elliptic flow” describes an emission pattern in which particles are found to be preferentially emitted with respect to a certain azimuthal angle and with back to back symmetry.

3.2 Time-Evolution

In order to define more clearly the most relevant quantities for collective motion in heavy-ion collisions, Figure 3.1 sketches schematically a typical heavy-ion reaction. When two nuclei approach each other, their orientation in space and the initial beam direction define the reaction plane. The impact parameter vector *b* is located in the reaction plane.

3.2.1 Initial Phase

When the two matter distributions approach each other and start to overlap, the properties of the NN interaction in free space will be visible in the scattering process. Nucleons at the surfaces will reflect the Lorentz-force-like behavior of the NN interaction most directly. They will be deflected outward and, because of symmetry for finite impact parameter, will show an enhancement in the reaction plane [1–5].

3.2.2 High Density Phase

Once the matter distributions of the projectile and_target overlap (Figure 3.1, *central row*), the properties of the NN interaction are not well known. At incident beam energies that exceed the velocity of sound in nuclear matter at ground-state nuclear-matter density (ρ_s= 2) [6], the nucleons_cannot escape fast enough and a zone of high density is formed. Many-body effects that are present even at normal nuclear-matter densities can occur, as well as modifications of the properties of the constituents (medium effects) [7, 8].

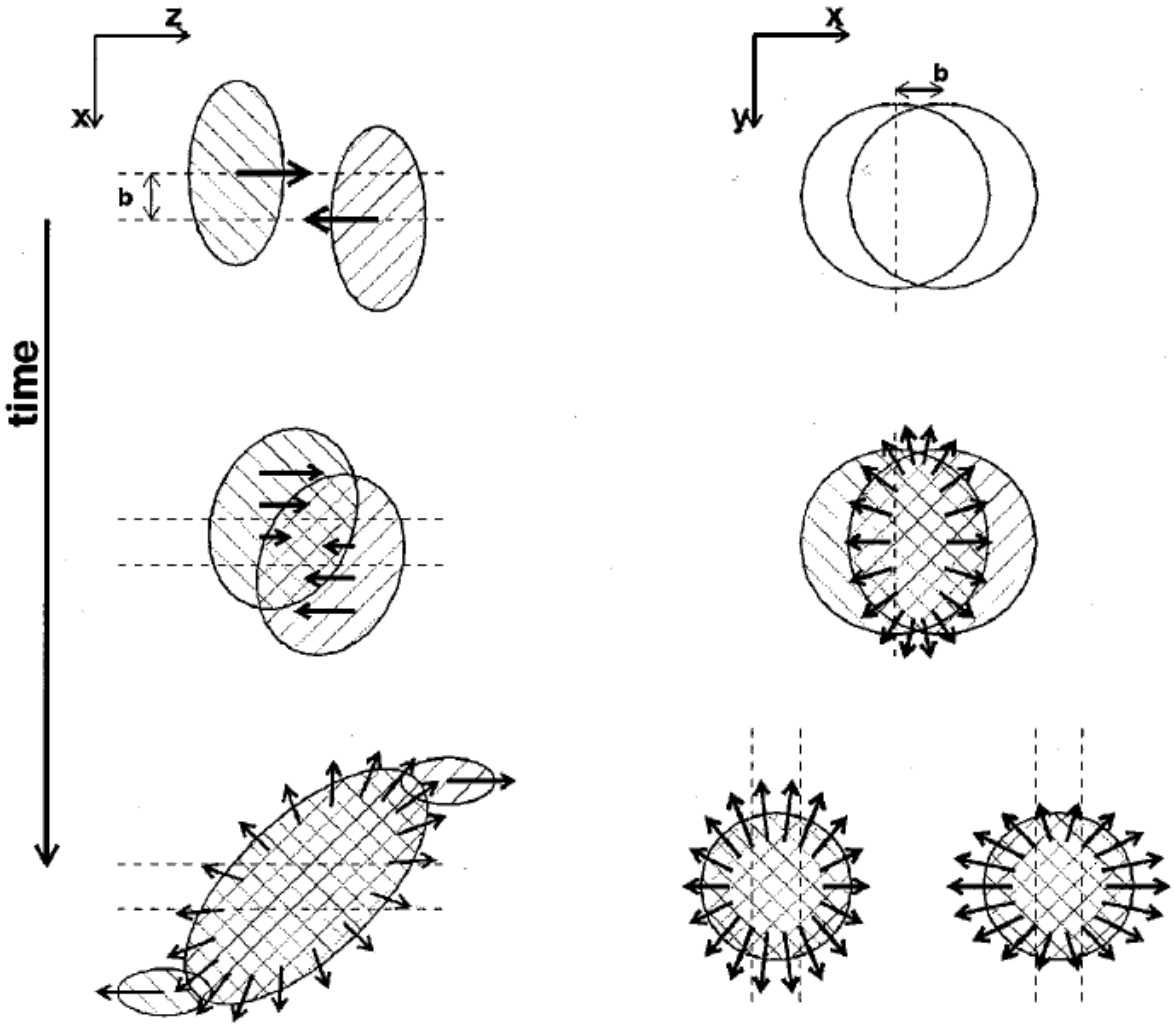

Fig 3.1 COLLECTIVE FLOW IN HEAVY-ION COLLISIONS : Schematic view of the time evolution in a heavy-ion collision and the development of collective velocity fields. Left, the time evolution of the reaction in the reaction plane. Right, a sketch of the transverse plane at midrapidity. Several phases of a typical heavy-ion reactions can be identified.

3.2.3 Expansion:

The next stage in the reaction scenario is the relaxation of the energy density. The central system is undergoing expansion, thereby reducing its temperature and density. For symmetry reasons, the expansion is azimuthally symmetric for central

collisions. For reactions with finite impact parameter, where an oriented velocity field might have survived the compression phase, the situation is much more complicated. The expansion now has a directed velocity field superimposed (Figure 3.1, *lower left*). The system always expands into the direction of the largest gradients in density and temperature. Inspection of the geometry depicted in Figure 3.1 reveals that, in transverse direction, the initial expansion is largest in the direction of the reaction plane. In longitudinal direction, the expansion scenario depends on the degree of stopping. For a high degree of stopping and given the fact that the nuclei are Lorentz contracted in this direction, the pressure gradient is largest along the beam direction; therefore, the system relaxes predominantly longitudinally.

3.2.4 Freeze-Out:

The reaction and the development of collective signatures, stops at a point commonly referred to as freeze-out. At this point the densities are small enough that during a typical path length no further interaction will occur. The properties of the system at freeze-out are quite well known from the systematic study of particle ratio.

3.3 Multi-fragmentation

Experiments have demonstrated that appropriately excited nuclear systems will undergo a multifragment disintegration leading to a final state composed of a mixture of fragments of charge $3 \leq Z \leq 30$ and light particles with $Z \leq 2$. Fragments are produced with large multiplicities in central heavy ion collisions at incident energies of $E_{beam}/A \leq 100$ MeV, in larger impact parameter heavy ion collisions at $E_{beam}/A \geq 200$ MeV, and in central light ion induced reactions at $E_{beam}/A \geq 5$ GeV [9].

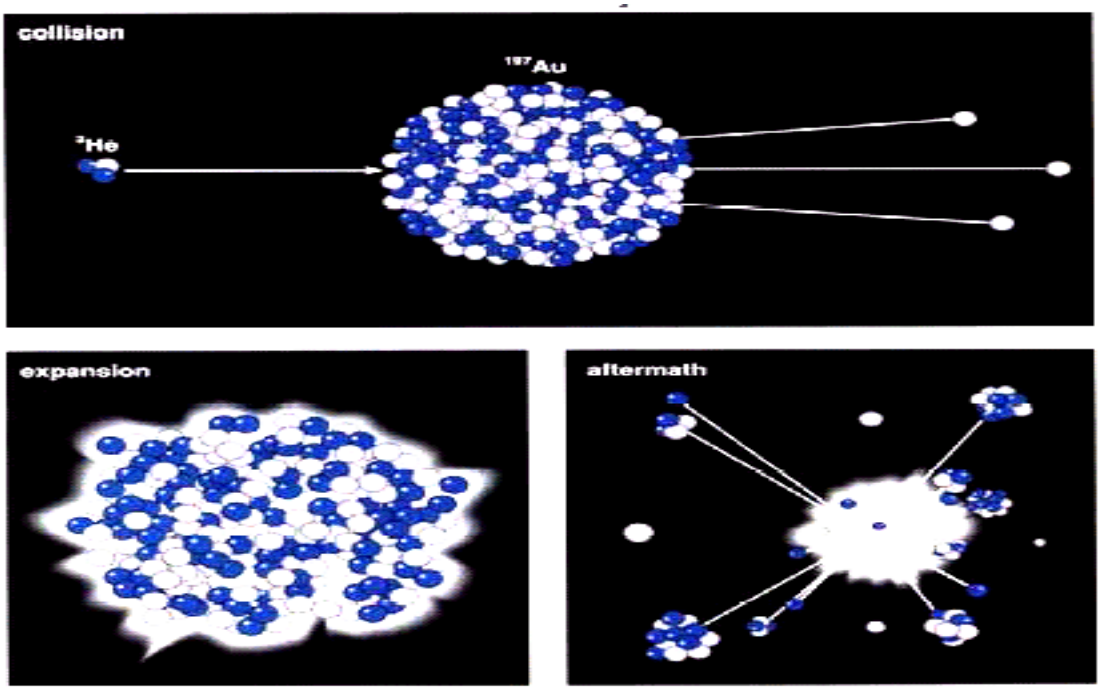

Fig3.2: multifragmentation at subnuclear density

3.4 Results and discussion

3.4.1 Effect of isospin on nuclear flow:

Anisotropic flow is defined as the different n-th harmonic coefficient v_n of the Fourier expansion for the particle invariant azimuthal distribution[14]

$$\frac{dN}{d\emptyset} \propto 1 + 2\sum_{n=1}^{\infty} v_n \cos(n\emptyset), \quad (3.1)$$

where $\emptyset$ is the azimuthal angle between the transverse momentum of the particle and the reaction plane. Note that the z-axis is defined as the direction along the beam and the impact parameter axis is labelled as x-axis. The first harmonic coefficient v_1

represents directed flow $v_1 = \langle \cos(2\emptyset) \rangle = \langle \frac{p_x}{p_T} \rangle$, where $p_T = \sqrt{p_{x+}^2} p_y^2$ is transverse momentum. While v_2 measure the eccentricity of the particle distribution in the momentum space represents the elliptical flow.

$$V_2 = \langle \cos(2\emptyset) \rangle = \langle \frac{p_x^2 - p_y^2}{p_t^2} \rangle \quad (3.2)$$

In the present analysis, thousands of events were stimulated for neutron rich systems $^{52}Cr_{24}$ + $^{108}Ag_{47}$, $^{45}Sc_{21}$+ $^{115}In_{49}$, $^{48}Ti_{22}$ + $^{112}Cd_{48}$, $^{59}Co_{27}$ + $^{101}Ru_{44}$, $^{72}Ge_{32}$ + $^{88}Sr_{38}$, and $^{75}As_{33}$ + $^{85}Rb_{37}$ between incident energy 50 and 300 MeV/nucleon using soft equation of state along with Cugnon cross-section. The collision geometry is non central with impact parameter $\hat{b} = .3$ .The sum total of the mass of the colliding nuclei is 160. Here our aim is to vary the number of neutrons and protons, but keep the total number of nucleon same.

The present analysis will be carried out in the frame work of isospin quantum molecular dynamics (IQMD) model. Results have been displayed at time 300 fm/c.

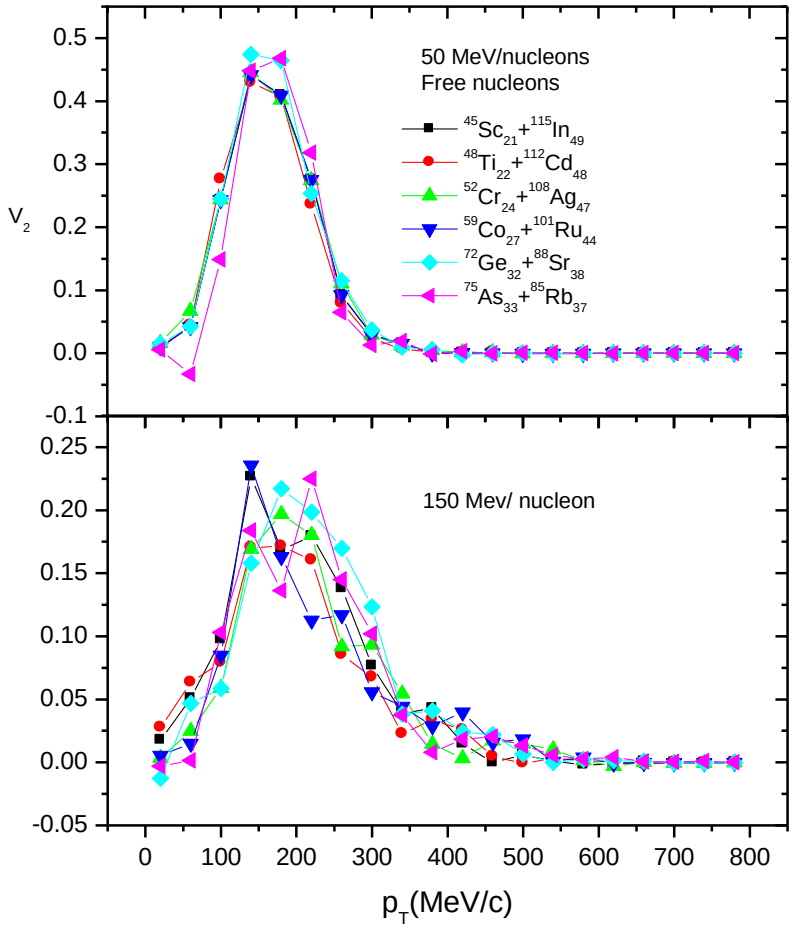

Fig 3.3: V_2 as function of p_t for different collision systems, at different energy for free nucleons.

Fig 3.3 displays the elliptical flow (v_2) as a function of transverse momentum p_T. Here we have varied the projectile mass from 45 to 75 to see the effect of isospin on elliptical flow. Since the energy of the reaction is low, so most of the collision are blocked due to pauli effect. This result in not much difference in elliptical flow values for different target and projectile combination. But if we look at the result carefully one can see that peak of free nucleons is shifted to higher values with increase in the size of projectile. Same trend is followed by LMF's. As the size of the projectile approaches the size of target more number of nucleon will suffer a collision and hence nucleon will

move in the direction transverse to the beam direction. The fluctuations are due to poor statistics.

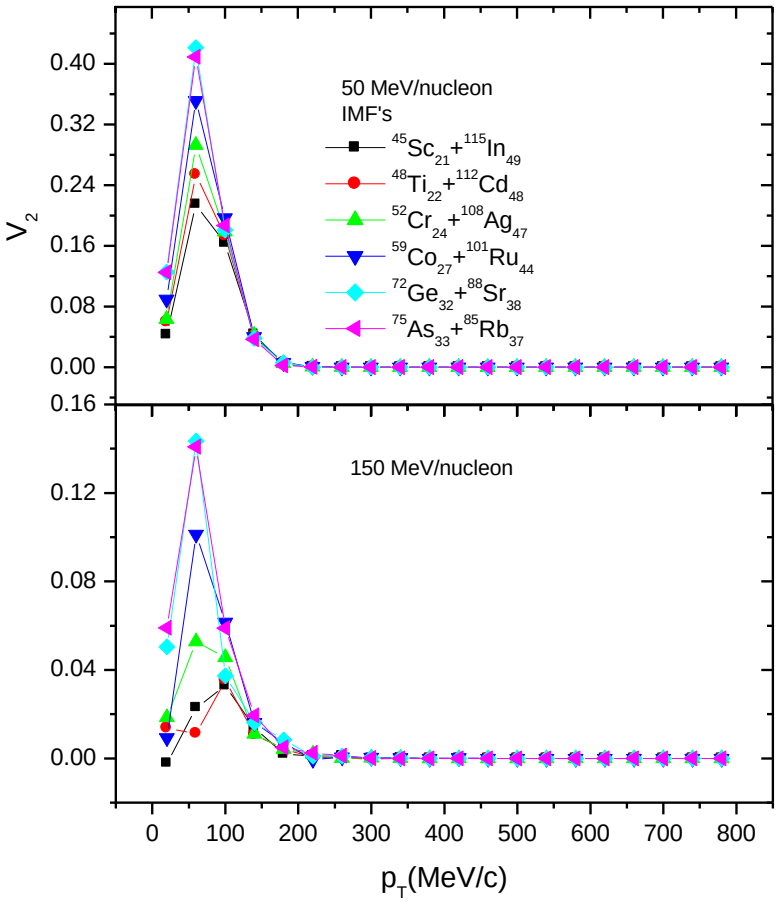

Fig 3.4 variation of V_2 with p_t for IMF's

In fig.3.4, the elliptical flow associated with IMF's has been displayed (upper panel at 50 MeV/nucleon and lower panel at 150 MeV/nucleon). Since the production of IMF's increases with mass of colliding nuclei, one can see that the elliptical flow (V_2) also show increase with increase in mass of the projectile. As one move from asymmetric to symmetric reaction, the elliptical flow increases because of increase in number of collisions. Also, if we compare upper panel with lower panel the flow associated with IMF's at 150 MeV/nucleon (lower panel) decreases as compared at 50 MeV/nucleon (upper panel). This is because at higher energy the destruction of nuclear

matter takes place and hence less number of IMF's are produced at same colliding geometry.

3.4.2 Effect of charge asymmetry on multiplicity

In fig.3.5, we display multiplicity of different mass fragments (free, LMF's (2<A<4) and IMF's (5<A<A_t/6)) obtained in final stage of reaction at different energies.

Since we kept total number of nucleons fixed, but varied the mass of the projectile. The effect of size asymmetry as the multiplicity of the fragments/Free nucleons have been studied here. The excited compound nucleus decays by emission of nucleons and fragments. As a result free nucleons, LMF's show a rise up to 150 MeV/nucleon then become constant. Heaviest projectile show largest number of LMF's compared to lightest projectile. This shows that LMF's are produced in midrapidity region due to nucleon-nucleon collisions. However, the IMF emission either is due to the spectator matter or serves as a counterbalancing of the attractive and repulsive forces; therefore, after reaching a boiling off point in the $^{45}Sc_{21}$+ $^{115}In_{49}$, $^{48}Ti_{22}$ + $^{112}Cd_{48}$, $^{52}Cr_{24}$ + $^{108}Ag_{47,}$ $^{59}Co_{27}$ + $^{101}Ru_{44}$, $^{72}Ge_{32}$ + $^{88}Sr_{38}$, and $^{75}As_{33}$ + $^{85}Rb_{37}$ reactions (typical IMF's are the remnant of projectile and target), it again drops down. One can also see that isospin asymmetry due to different number of protons in projectile nucleon play significant role in the production of Free, LMF's and IMF's. A clear rise and fall in the multiplicities of IMF's is observed with an increase in the incident energy.

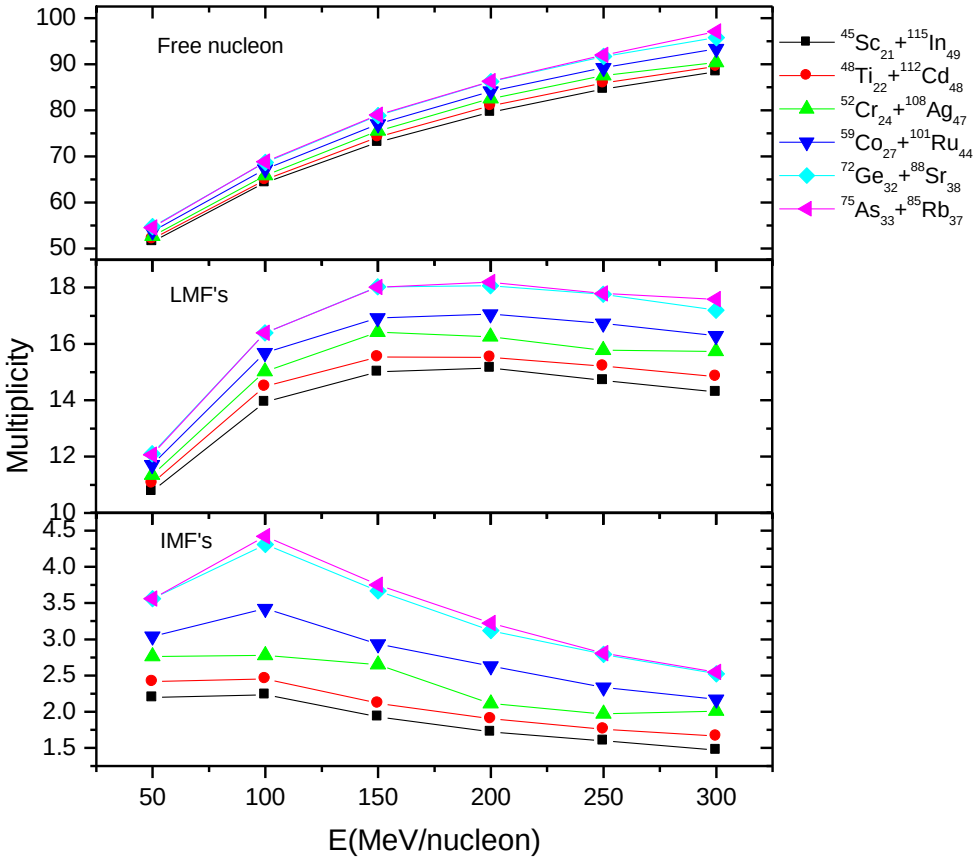

Fig 3.5: Multiplicity as a function of energy for different fragments.

3.5 References

[1] Norbert Herrmann, Johannes P.Wessels, and ThomasWienold, Annu. Rev. Nucl. Part. Sci. 1999. 49:581–632.

[2]. Gale C, Bertsch G, DasGupta S. *Phys. Rev.C* 35:1666 (1987).

[3]. Aichelin J, et al. *Phys. Rev. Lett.* 58:1926 (1987).

[4]. Blaattel B, et al. *Phys. Rev.C*43:2728 (1991).

[5]. Greiner W, Staocker H. *Phys. Rep.* 137:277 (1986).

[6]. Braun-Munzinger P, Stachel J, Wessels JP, Xu N. *Phys. Lett.* B344:43 (1995).

[7]. Braun-Munzinger P, Stachel J,Wessels JP, Xu N. *Phys. Lett.* B365:1 (1996).

[8]. Physical Review C 68, 034609 (2003).

[10]. Jatinder Kaur Dhawan Ph.D. Thesis PU Chandigarh (2007).

[11]. Suneel Kumar Ph.D Thesis P U, Chandigarh (1999).

[12]. A. Schauttauf et al., Nucl. Phys. A 607 (1996) 457.

[13] J. Pochodzalla et al., Phys. Rev. Lett. 75 (1995) 1040.

[14].Y. T Zhi, M. Y. Gang, C. X. Zhou, F. D. Qing, G. Wei, M. C. Wang, S. W. Qing, T. W. Dong, and W. Kun, arXiv:0709.1244v1 [nucl-th] 9 Sep 2007

CHAPTER 4

EFFECT OF CROSS-SECTION ON NUCLEON-NUCLEON COLLISION

4.1 Introduction

In nuclear physics and particle physics, the concept of a cross section is used to express the likelihood of interaction between particles. When particles are thrown against a foil made of a certain substance, the *cross section* is a hypothetical area measured around the target particles that represents a surface of a nucleus is used to characterize the probability of collision.

4.2 Different types of NN cross-section

The dynamics of the reaction is governed by the mean field (or mutual two and three body interactions) and by nucleon nucleon cross section. Both these ingredient have different domain of dominance. At low energies, the two body collisions are nearly absent and therefore, the mean field (mutual two and three body interaction dominates the reaction where as the nucleon nucleon collisions take over the picture at intermediate and relativistic energies.

At low energies, the mean free nucleon nucleon cross section increases from 1 mb to 10 mb. At low energies, the NN collisions are blocked by Pauli principle. Hence the free scattering cross section should be replaced by the in medium cross-section. Due to lack of any reliable calculation, a constant cross section of 10 mb was used in the past. At low energies, the impact of NN collision is small. This impact increases with increase in the bombarding energy [1, 2].

During the propagation, two nucleons can collide if they come closer than a certain distance. The scattering of these nucleons is dominated by a Monte Carlo

procedure which is a stochastic scattering and hence is different from Rutherford scattering. For NN cross section σ, one can use a simple parameterisation which depends on the centre of mass energy of nucleons [3]. A more realistic cross section which takes care of the isospin of resonance and decay of resonance was also available. In most of the parameterizations of the NN cross section, the following processes are always there:

$$N + N \rightarrow N + N, \quad (4.1)$$

$$N + N \rightarrow N + \Delta, \quad (4.2)$$

$$N + N \rightarrow \Delta + \Delta, \quad (4.3)$$

$$N + \Delta \rightarrow N + N, \quad (4.4)$$

$$\Delta \rightarrow N + \pi, \quad (4.5)$$

$$N + \Delta \rightarrow N + \Delta, \quad (4.6)$$

$$\Delta + \Delta \rightarrow \Delta + \Delta. \quad (4.7)$$

The phase space of scattered nucleon is checked with so called classical Pauli-blocking method. No collision takes place if the phase space of scattered nucleons is already forbidden. In the following, we first describe different nucleon nucleon cross - sections which will be used in present analysis.

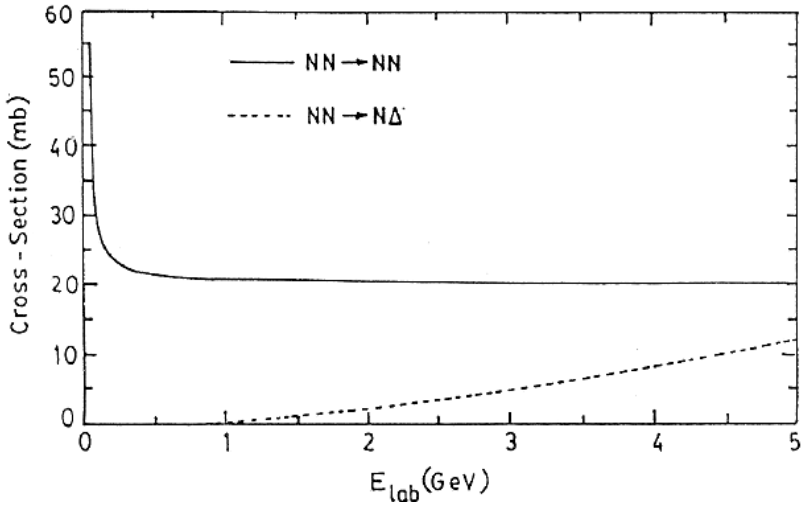

Fig 4.1 The Cugnon parameterization for the elastic (solid line) and inelastic (dashed line) cross-sections of nucleon-nucleon scattering as a function of the incident energy (E_{lab})[5].

4.2.1. Energy dependent cross section

Very popular and widely used cross-section was derived by Cugnon *et a [5]* which is a parametric fit on the experimental data. Here cross-section is divided into elastic and inelastic parts which depend on the center-of-mass energy available to the colliding pair of nucleons. For elastic channels, we use the total and differential cross-section with $\sqrt{s}$, the NN centre of mass energy given by:

$$\sigma_{nn}^{(el)}(\sqrt{s}) = \begin{cases} 55(\text{mb}), & \text{if } \sqrt{s} < 1.8993; \\ \dfrac{35}{1 + 100(\sqrt{s} - 1.8993)} + 20, & \text{if } \sqrt{s} \geq 1.8993; \end{cases}, \qquad (4.8)$$

the nucleon-nucleon center-of-mass energy given by

$$\sqrt{s} = \sqrt{(E_{1+}E_2)^2 - (p_1 + p_2)^2}. \qquad (4.9)$$

.

For inelastic channels, the total cross-section is parameterized as:

$$\sigma_{mn\to n\Delta}^{(in)}(\sqrt{s}) = \begin{cases} 0, & (1) \\ \dfrac{20(\sqrt{s} - 2.015)^2)}{0.015 + (\sqrt{s} - 2.015)^2}, & (2) \end{cases} \qquad \begin{matrix} \text{if } \sqrt{s} < 2.015 & (1) \\ \text{if } \sqrt{s} \geq 2.015 & (2) \end{matrix} \Bigg\}, \qquad (4.10)$$

The angular distribution for inelastic channels is assumed to be isotropic.

The elastic and inelastic parts of the cross-section are displayed in Fig.4.1. The elastic cross-section falls sharply and saturates around 20 mb. Whereas, the inelastic cross- section increases linearly with bombarding energies. At very high energies, the nucleon- nucleon cross-section is fully dominated by the inelastic channel.

4.2.2 Constant cross section

At intermediate energies, several calculations are reported where a constant section have been also used. Here we also use an isotropic and energy independent NN cross section $б_{nn}$ = 55, 40, and 20 mb, respectively.

4.3 Isospin dependence of free-space N-N cross sections

It is well-known that the scattering cross section between two nucleons depends on their isospin [6]. Fig. 4.2 compares the free-space cross sections for neutron-proton and proton-proton or neutron-neutron scattering as functions of bombarding energy. The data in the energy range of 10 MeV/nucleon ≤ E_{lab} ≤ 1000 MeV/nucleon can be parameterized by [7]

$$\sigma_{np}^{free} = -70.67 - 18.18\,\beta^{-1} + 25.26\,\beta^{-2} + 113.85\,\beta \quad \text{(mb)}, \tag{4.11}$$

$$\sigma_{pp}^{free} = 13.73 - 15.04\,\beta^{-1} + 8.76\,\beta^{-2} + 68.67\,\beta^{4}\,\text{(mb)}, \tag{4.12}$$

where β ≡ v/c is the velocity of the projectile nucleon. It is seen that below about 500 MeV the neutron-proton cross section is about a factor of 2 to 3 higher than the proton proton or neutron-neutron cross section.

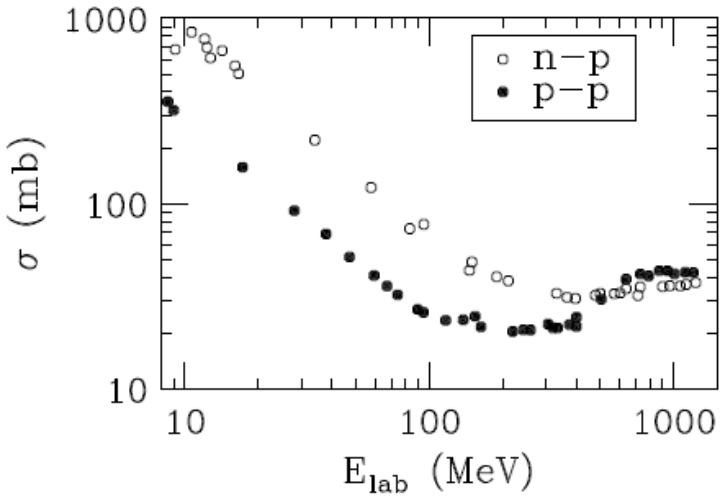

Figure 4.2: Cross sections of neutron-proton and proton-proton scatterings as function of bombarding energy [8].

4.4 Results and discussion

4.4.1 Effect of cross-section on elliptical flow

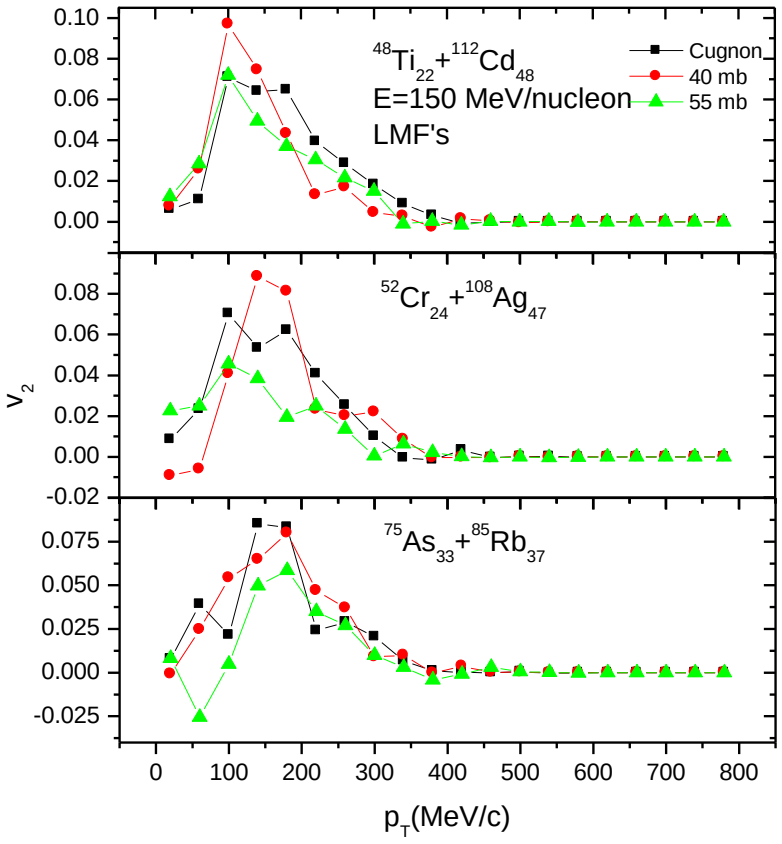

Fig 4.3 Elliptical flow as function of transverse momentum with different cross-section for three different system $^{48}Ti_{22}+ ^{112}Cd_{48}$, $^{52}Cr_{24} + ^{108}Ag_{47}$ and $^{75}As_{33}+^{85}Rb_{37}$ (LMF's)

Fig.4.3 presents the elliptical flow $\langle V_2 \rangle$ [9] associated with LMF's as function of transverse momentum p_t for with different cross-section for three different system $^{48}Ti_{22}+ ^{112}Cd_{48}$, $^{52}Cr_{24} + ^{108}Ag_{47}$ and $^{75}As_{33}+^{85}Rb_{37}$.

Here simulations are carried out for non central collision at incident energy 150 MeV/nucleon.

$\langle V_2 \rangle$ due to Cugnon cross-section is smaller than its value at 55 mb and 40 mb. This is due to the fact that at smaller cross-section few particles suffer the collision. But as the mass of projectile increases and target decreases, the picture changes. The $\langle V_2 \rangle$ due to 40 mb and 55 mb start approaching the $\langle V_2 \rangle$ due to Cugnon cross-section.

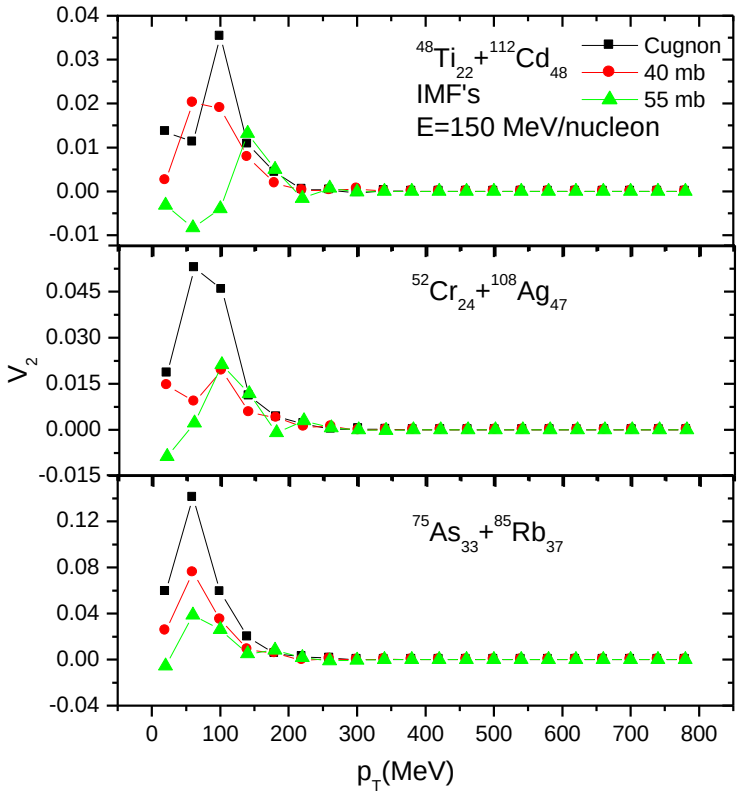

Fig 4.4 Elliptical flow as function of transverse momentum with different cross-section for three different system $^{48}Ti_{22}+^{112}Cd_{48}$, $^{52}Cr_{24}+^{108}Ag_{47}$ and $^{75}As_{33}+^{85}Rb_{37}$ (IMF's)

The $\langle V_2 \rangle$ due to IMF's shows the opposite picture. The $\langle V_2 \rangle$ due to Cugnon is larger than $\langle V_2 \rangle$ due to 40 mb and 55 mb. This is because if system suffers less number of collisions then more the correlation more the nucleons are produced. Thus

$<V_2>$ is more. Also the peak value of $<V_2>$ due to IMF's increases as target and projectile size asymmetry decreases.

4.4.2 Effect of cross-section on nuclear stopping

The degree of stopping in heavy-ion collisions is an important quantity in determining the outcome of a reaction. It is usually studied by measuring the rapidity distribution or the asymmetry of the nucleon momentum distribution. The effects of both N -N cross section on colliding systems with different neutron proton ratios in the beam energy ranging from 50 MeV/nucleon to 300 MeV/nucleon have been studied using an isospin dependent quantum molecular dynamics (IQMD) model. Soft equation of state has been used in the present analysis.

The following two quantities can be used to describe nuclear stopping in HIC. The momentum quadrupole Q_{ZZ} defined as [10]

$$Q_{zz} = \sum_i^A \left(2P_z(i)^2 - P_x(i)^2 - P_y(i)^2\right) \quad (4.13)$$

and the transverse-parallel ratio of momentum R given by

$$R=\left(\frac{2}{\pi}\right),\left(\sum_i^A P\perp(i)/\left(\sum P\parallel(i)\right)\right) \quad (4.14)$$

Here the total mass A is the sum of the projectile mass A_p and the target mass A_t. The values of the transverse and parallel components of the momentum of i^{th} nucleon are:

$$P_\perp(i) = \sqrt{P_x(i)^2 + P_y(i)^2}\ and\ P_\parallel(i) = P_z(i), \text{ respectively.} \quad (4.15)$$

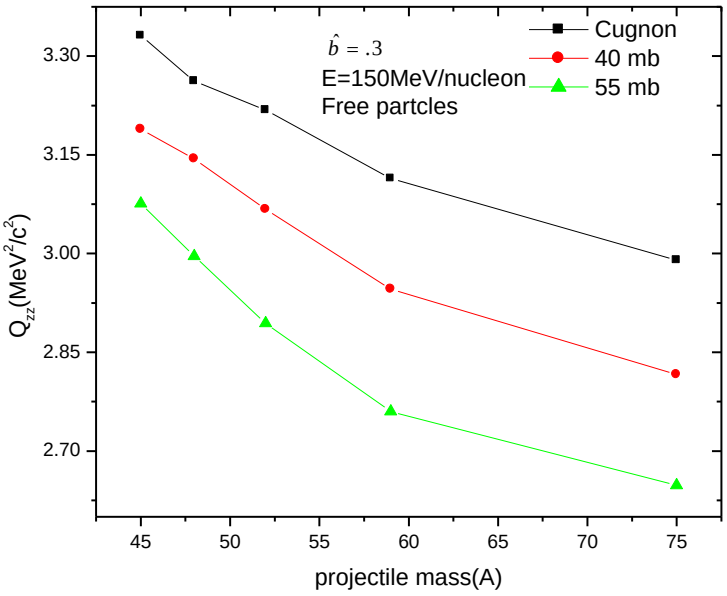

Fig 4.5 Q_{zz} as function of mass of projectile(A) ranging from 45 to 75, at E 150 MeV/nucleon.

Fig 4.5: First of all, we study the effect of isospin and cross-section on Q_{zz} of free particle emissions at energy 150 MeV/nucleon. Here mass of projectile varies from 45 to 75. We observe that the value of Q_{zz} decrearses with increase of projectile mass. As the mass of the projectile approaches mass of target, the stopping start increasing or value of Q_{zz} start decreasing. Trend followed for different cross-sections is similar. But for Cugnon cross-section, value of Q_{zz} is higher as compared to its value at 40 mb and 55mb, means less stopping at low cross-section compared to high cross-section. This is because at large cross-section more number of collisions takes place and hence the stopping factor will decrease. Also when size of target and projectile become comparable we get maximum stopping of least value of Q_{zz}.

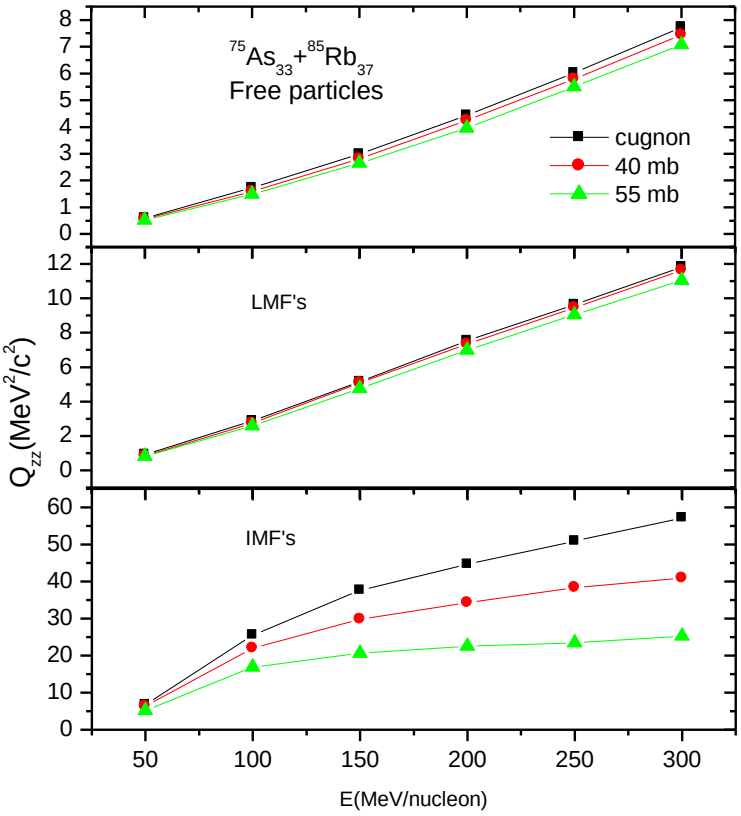

Fig 4.6 Shows the variation of Q_{zz} as function of energy at different cross sections.

In fig.4.6. the value of Q_{zz} for free nucleons, LMF's and IMF's increases with incident energy. Larger cross-section we get smaller value of $Q_{zz.}$ This is because at larger cross-section nucleon suffer more collision and deflect from their path which gives larger value of x and y component of momentum. Also with the increase in energy the violence of collision also increases. The z-component of momentum become stronger than x and y component and hence the value of Q_{zz} increases, means stopping decreases.

Fig 4.7 displays the variation of stopping (R) as function of energy for $^{75}As_{33}+^{85}Rb_{37}$ for different cross sections. Upper window is for free nucleon, middle for LMF and lower for IMF. For complete stopping value of R should be equal to one. But as the energy increases the p_z become stronger than p_x and p_y so the net value of R

decreases indicate less stopping. From this figure again one thing is clear that at large cross-section stopping is more than smaller cross-section. Moreover at low energy stopping is more significant than at higher energy. Trend followed is same in all three windows showing significance of isospin dependence of cross-section on stopping.

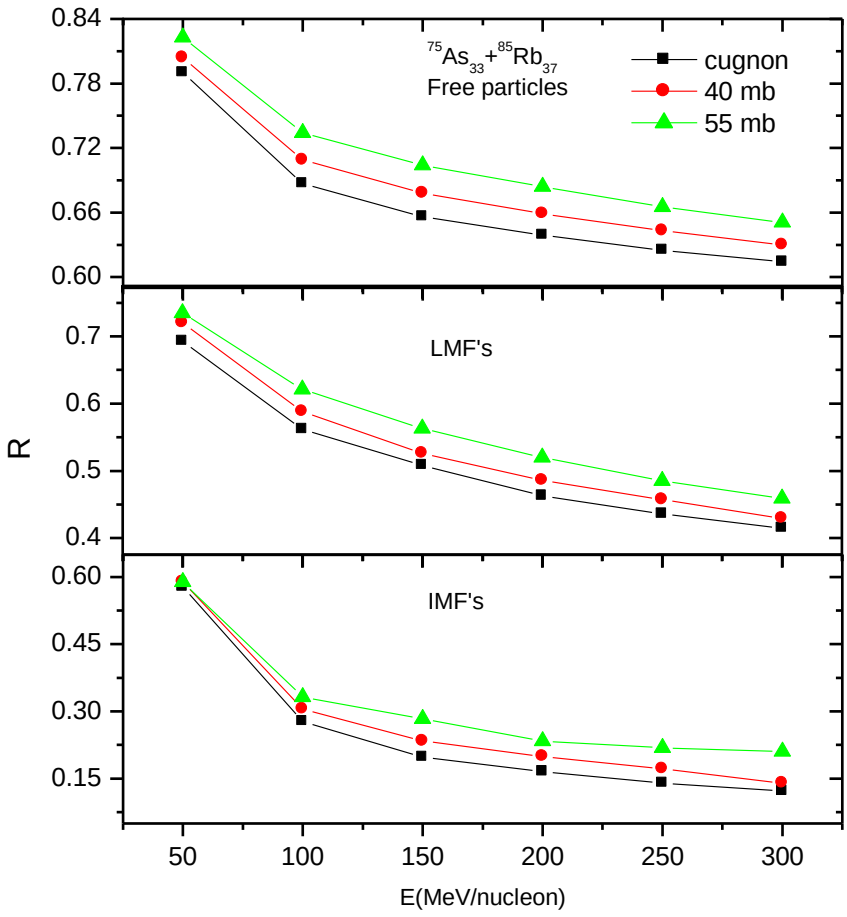

Fig 4.7 stopping as function of energy at different cross sections with b=.3 fm for $^{75}As_{33}+^{85}Rb_{37}$.

4.4.3 Effect of cross-section on multiplicity

We here present the calculations of effect of different cross-sections on multifragmentation. We have stimulated the reactions of $^{48}Ti_{22}+ {}^{112}Cd_{48}$, $^{52}Cr_{24} + {}^{108}Ag_{47}$ and $^{75}As_{33}+ {}^{85}Rb_{37}$ for central collision at energies between 50 and 300 MeV/nucleon.

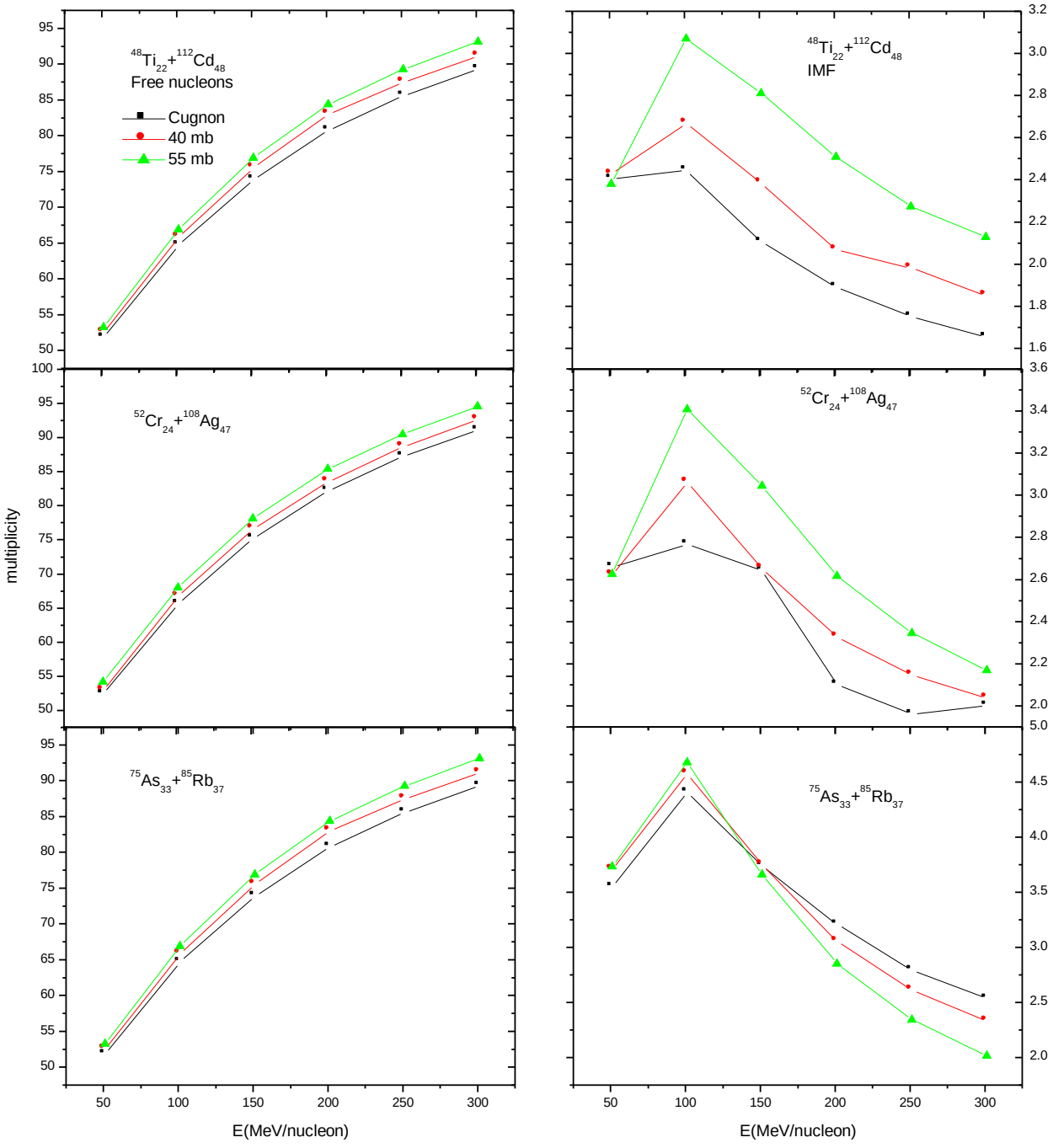

Fig 4.8(above), L.h.s shows multiplicity of free nucleon and on (R.h.s) is multiplicity of IMF's as a function of energy.

In fig 4.8, we display the multiplicity of free as function of energy on left hand side panel and that of free nucleons on right hand side of panel. In all cases we clearly see effects of NN cross-section. In case of free nucleons multiplicity increases with increase of incident energy and shows higher value for larger cross-section. On the other hand, one can see a rise and fall in the multiplicity of IMF's, behaviour is similar to the behaviour predicted by Aladin group. This is due to non central collision; it generates better repulsion, and the frequent NN collisions occurring at these energies very less IMF's production. Hence we can see a fall in the production of IMF's. With the increase of incident energy NN collision also increases which result in the production of free particles and LMF's as compared to IMF's at lower energies many of the collisions are pauli blocked hence multiplicity is smaller at smaller energies.

4.5 References

[1]. Suneel Kumar, Ph.D thesis PU Chandigarh (1999).

[2]. S. Kumar and R. K. Puri. Physical Review C volume 58, number 3, September 1998

[3]. H. Huber and J. Aichelin, Nucl. Phys. A 573, 587 (1994).

[4]. S. W. Huang, Ph.D. Thesis, University of TÄubingen, TÄubingen, Germany (1994).

[5]. J. Cugnon, T. Mizutani and J. Vandermeulen, Nucl. Phys. A 352, 505 (1981).

[6]. B. A. Li, C. M. Ko and W. Bauer, arXiv:nucl-th/9707014v1 7 Jul 1997.

[7]. S.K. Charagi and S.K. Gupta, Phys. Rev. C41, 1610 (1990).

[8]. G. Alkahzov et al., Nucl. Phys. A280, 365 (1977).

[9]. Y. T.-Zhi, M. Y.-Gang, C. X. Zhou, F. D. Qing, G. Wei, M. C.Wang, S. W.Qing, T. W. Dong, and W. Kun, arXiv:0709.1244v1 [nucl-th] 9 Sep 2007.

[10]. J.Y Liu, W. J. Guo, S. J. Wang, W. Zuo, Q. Zhao, and Y. F. Yang, Phys. Rev. Lett. 86.975

Chapter 5

Summary

"We used to think if we knew one, we knew two, because one and one are two. We are finding that we must learn a great deal more about `and' "..... Sir Arthur Eddington (1882-1944).

This thesis contains a theoretical study of effect of isospin on nucleon-nucleon collisons and its related phenomena like nuclear flow, multifragmantation, and nuclear stopping in heavy-ion collisions at intermediate energies. The *Isospin Quantum Molecular Dynamics (IQMD)* model was used to generate the data. In chapter 1, we have discussed isospin, nuclear physics at intermediate energy and we have gone through the experimental and theoretical review.

The details of various theoretical models were discussed in Chap. 2. We discussed, in particular, the Isospin Quantum Molecular Dynamics (IQMD) model used for the present study.

In chap.3, we investigated the effect of isospin on nuclear flow and effect of charge asymmetry on multiplicity in heavy-ion collisions. In the present analysis, thousands of events were stimulated for neutron rich systems $^{52}Cr_{24}$ + $^{108}Ag_{47}$, $^{45}Sc_{21}$+ $^{115}In_{49}$, $^{48}Ti_{22}$ + $^{112}Cd_{48}$, $^{59}Co_{27}$ + $^{101}Ru_{44}$, $^{72}Ge_{32}$ + $^{88}Sr_{38}$, and $^{75}As_{33}$ + $^{85}Rb_{37}$ between incident energy 50 and 300 MeV/nucleon using soft equation of state along with Cugnon cross-section. The collision geometry is semi central with impact parameter $\hat{b} = 0.3$. We observe that elliptical flow decreases with rise in energy and it increases as the mass of projectile changes from 52 to 72. It is clearly observed that transverse flow is sensitive to the asymmetry of the colliding nuclei.

. For free nucleons, LMF's, and IMF's the multiplicity increases with the increase in the mass of projectile nuclei.

In chap.4, we studied the effect of cross-section on elliptical flow, nuclear stopping and multiplicity for three different system $^{48}Ti_{22}$+ $^{112}Cd_{48}$, $^{52}Cr_{24}$ + $^{108}Ag_{47}$ and $^{75}As_{33}$+$^{85}Rb_{37.}$ We observe that the value of elliptical flow v_2 as function of p_t is smaller for Cugnon cross-section as compared to 40 mb and 55 mb for all three systems. We have found that value of elliptical flow significantly depends on cross-section.

In case of $Q_{zz,}$ observe that the value of Q_{zz} decrearses with increase of projectile mass. Trend followed for different cross-sections is similar. But for Cugnon cross-section, value of Q_{zz} is higher as compared to its value at 40 mb and 55mb. Also as the beam energy increases, the Q_{zz} increases and for larger cross-section we get smaller value of Q_{zz} means more stopping.

At last we discussed that in case of free nucleons multiplicity increases with increase of incident energy and shows higher value for larger cross-section. On the other hand, one can see a rise and fall in the multiplicity of IMF's.